

000 001 002 003 004 005 SO-FAKE: BENCHMARKING SOCIAL MEDIA IMAGE 006 FORGERY DETECTION 007 008 009

010 **Anonymous authors**
011 Paper under double-blind review
012
013
014
015
016
017
018
019
020
021
022
023
024
025
026
027
028
029
030

031 ABSTRACT

032 Recent advances in AI-powered generative models have enabled the creation of
033 increasingly realistic synthetic images, posing significant risks to information
034 integrity and public trust on social media platforms. While robust detection frame-
035 works and diverse, large-scale datasets are essential to mitigate these risks, existing
036 academic efforts remain limited in scope: current datasets lack the diversity, scale,
037 and realism required for social media contexts, and evaluation protocols rarely
038 account for explanation or out-of-domain generalization. To bridge this gap, we
039 introduce **So-Fake**, a comprehensive social media-oriented dataset for forgery
040 detection consisting of two key components. First, we present **So-Fake-Set**, a
041 large-scale dataset with over **2 million** photorealistic images from diverse gener-
042 ative sources, synthesized using a wide range of generative models. Second, to
043 rigorously evaluate cross-domain robustness, we establish **So-Fake-OOD**, a novel
044 and large-scale (**100K**) out-of-domain benchmark sourced from real social media
045 platforms and featuring synthetic imagery from commercial models explicitly ex-
046 cluded from the training distribution, creating a realistic testbed that mirrors actual
047 deployment scenarios. Leveraging these complementary datasets, we present **So-
048 Fake-R1**, a baseline framework that applies reinforcement learning to encourage
049 interpretable visual rationales. Experiments show that So-Fake surfaces substantial
050 challenges for existing methods. By integrating a large-scale dataset, a realistic
051 out-of-domain benchmark, and a multi-dimensional evaluation protocol, So-Fake
052 establishes a new foundation for social media forgery detection research.
053

1 INTRODUCTION

034 The rapid evolution of generative AI (Shuai et al., 2024; Hu et al., 2025) has made it increasingly
035 difficult to verify the authenticity of social media images, as it enables malicious actors to create
036 deceptive content that misleads public opinion or spreads false information. This has motivated
037 the creation of large-scale datasets to study and improve forgery detection. In recent years, several
038 deepfake datasets (Yan et al., 2024; Bhattacharyya et al., 2024; Zhu et al., 2023) have been proposed
039 to train more robust forgery detection models. However, they generally exhibit three significant
040 limitations that make them inadequate for addressing the complex challenges of social media image
041 forgery detection: **1) Narrow Categorical Scope**. Existing datasets (Ricker et al., 2024; Peng et al.,
042 2024; Yang et al., 2023) focus narrowly on specific categories such as faces, animals, or humans,
043 failing to represent complex real-world social media contexts. **2) Outdated Generation Quality**.
044 Most datasets (Zhu et al., 2023; Corvi et al., 2023; Huang et al., 2024b) rely on outdated generation
045 techniques, which result in less convincing forgeries that are easier for both humans and models
046 to detect. **3) Limited Cross-Domain Evaluation**. Existing datasets lack established protocols for
047 measuring cross-domain generalization and rarely include a dedicated out-of-distribution benchmark.
048 While recent works (Ricker et al., 2024; Huang et al., 2025b; Dell’Anna et al., 2025) have attempted
049 to introduce forgery detection datasets for social media images, they face significant constraints
050 in acquiring authentic platform content. Existing benchmarks approximate social media imagery
051 indirectly, for instance by re-uploading generated images or substituting generic open datasets. These
052 proxies fail to capture the fidelity, compression, and topical diversity of authentic social media content,
053 highlighting the need for datasets that more faithfully reflect real-world conditions.

Beyond dataset limitations, existing evaluation protocols also remain inadequate. Social media
forgeries range from fully synthetic to regionally tampered images (Huang et al., 2025b), which

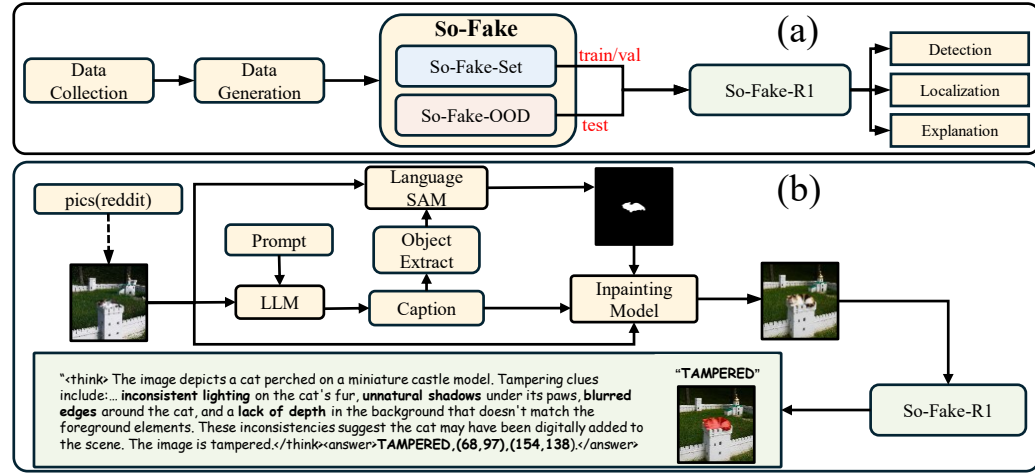


Figure 1: **(a) Overview.** So-Fake comprises So-Fake-Set (train/val) and So-Fake-OOD (test), which together enable evaluation of detection, localization, and explanation with So-Fake-R1. **(b) Illustrative Example.** A real image from the subreddit *pics* is captioned by an LLM, combined with Language SAM and an inpainting model to produce tampered samples. So-Fake-R1 then analyzes the manipulated image and outputs the class label, localized region, and an interpretable rationale.

calls for benchmarks that evaluate not only detection but also manipulation localization and explanation to foster user trust. Despite progress, most methods remain limited: many target only face deepfakes as binary classification (Yan et al., 2024; 2023; Kroiß & Reschke, 2025), or extend to mask prediction (Dong et al., 2023; Guo et al., 2023; Zhang et al., 2024), yet provide little insight into their decisions. This black-box nature further limits applicability in social media, where diverse manipulations demand transparent explanations. To address this challenge, recent advances in large language models (Li et al., 2025; Kang et al., 2025; Xu et al., 2024; Ji et al., 2025) have inspired explainability methods that generate human-readable rationales, but these depend on costly human annotations and cannot jointly address tampered and fully synthetic cases. Consequently, existing methods and protocols remain inadequate for social media forgeries, highlighting the need for joint evaluation of detection, localization, and explanation to ensure trustworthiness.

To address these limitations, we introduce **So-Fake**, a comprehensive benchmark for social media forgery detection with explicit protocols for evaluating detection, localization, and explanation. As illustrated in Figure 1, it consists of two complementary components. **So-Fake-Set** is the main training and validation corpus, comprising over **2M** images across **12** diverse categories (see Figure 2 (a) and Figure 3 (a)) and extending beyond traditional face-centric datasets to include humans, animals, and events. **So-Fake-OOD** is a **100K**-image out-of-distribution benchmark that pairs authentic social media content from Reddit¹ with synthetic imagery generated by leading commercial models listed in the Leaderboard². The **30** generation and manipulation methods in So-Fake-Set are entirely disjoint from the **10** commercial models in So-Fake-OOD (see Figure 2 (b)), reflecting the closed-source nature of many real-world tools and enabling realistic evaluation of generalization to unseen generators. In both datasets, images are labeled as real, tampered, or full synthetic, reflecting the major forms of fake content encountered on authentic social media environments.

Leveraging these complementary datasets, we further provide **So-Fake-R1**, a baseline framework that illustrates the practical use of So-Fake for social media forgery detection. So-Fake-R1 leverages reinforcement learning (RL) to produce interpretable predictions, enabling comprehensive evaluation across detection, localization, and explanation. The main contributions of this paper are as follows:

- We introduce **So-Fake**, a large-scale social media-oriented dataset comprising **So-Fake-Set** for training/validation and **So-Fake-OOD** for out-of-distribution evaluation.
- We propose **So-Fake-R1**, an RL-based framework that unifies detection, localization, and explanation of social media forgeries, thereby demonstrating the utility of So-Fake.
- Extensive experiments demonstrate So-Fake's effectiveness as a comprehensive benchmark, with So-Fake-R1 achieving state-of-the-art results across detection, localization, and explanation tasks while maintaining strong generalization to out-of-distribution domains.

¹<https://www.reddit.com>

²<https://artificialanalysis.ai/text-to-image>

108 Table 1: Comparison with recent image forgery datasets. “–” in #Methods indicates the number of
 109 generative methods was not specified; “–” in Latest Fake indicates the specific generative method
 110 was not specified; Column abbreviations: MultiCls = Multiclasses, Expl. = Explanation.

112	Dataset	Social Media	Latest Fake	#Methods	Data Sources	#Images	MultiCls	Mask	Expl.	OOD
113	ArtiFact ('23)	✗	Palette ('22)	25	COCO, FFHQ, LSUN	2M+	✗	✗	✗	✗
114	DMimage ('23)	✗	DALL-E ('22)	10	COCO, ImageNet	0.4M+	✗	✗	✗	✗
115	AIGCD ('23)	✗	Wukong ('22)	16	LSUN, COCO, FFHQ	0.7M+	✗	✗	✗	✗
116	SynthScars ('25)	✗	FLUX ('24)	-	RichHF-18K, Chameleon, FFAA	13K	✗	✓	✓	✗
117	FakeClue ('25)	✗	FLUX ('24)	-	GenImage, FF+++, Chameleon	0.1M+	✗	✗	✓	✗
118	GenImage ('23)	✗	Wukong ('22)	8	ImageNet	2M+	✗	✗	✗	✗
119	WildFake ('25)	✗	DALL-E 3 ('23)	27	ImageNet, COCO, FFHQ, LSUN, +3 more	3M+	✗	✗	✗	✗
120	Community Forensics ('25)	✗	FLUX ('24)	4803	LAION, ImageNet, COCO, FFHQ, +7 more	2M+	✗	✗	✓	✓
121	SID-Set ('24)	✓	FLUX ('24)	2	COCO, Flickr30k, MagicBrush	0.3M	✓	✓	✓	✗
122	Deepfake-Eval-2024 ('25)	✓	-	-	X, Tiktok, Instagram	1975	✗	✗	✗	✗
123	TrueFake ('25)	✓	FLUX ('24)	8	FFHQ, FORLAB, Facebook, X, Telegram	0.6M+	✗	✗	✗	✗
124	So-Fake	✓	Nana Banana ('25)	40	COCO, Flickr30k, WIDER, OpenForensics, Reddit, OpenImages, FFHQ, CelebA	2M+	✓	✓	✓	✓

2 RELATED WORK

2.1 IMAGE FORGERY DETECTION DATASETS

125 Early datasets such as DFFD (Dang et al., 2020), ForgeryNet (He et al., 2021), and FaceForen-
 126 sics++ (Rössler et al., 2019) established the foundation for deepfake detection research, albeit with
 127 a narrow emphasis on GAN-generated facial forgeries (Karras et al., 2020; 2021a). With the rise
 128 of diffusion models, research has expanded beyond facial manipulations to encompass broader
 129 AI-generated content (AIGC) detection. This trend is reflected in the emergence of recent bench-
 130 marks such as GenImage (Zhu et al., 2023) and DMimage (Corvi et al., 2023). As detection tasks
 131 increasingly target content circulating in real-world environments, attention has shifted towards
 132 constructing specialized datasets for social media forgery detection (Ricker et al., 2024; Huang et al.,
 133 2025b; Dell’Anna et al., 2025). Despite these advances, current datasets exhibit notable shortcomings,
 134 including reliance on outdated generative techniques and insufficient diversity in real-world scenarios.
 135 More recently, WildFake (Hong et al., 2025) collected millions of community-shared synthetic images
 136 from platforms, while Community Forensics (Park & Owens, 2025) systematically sampled from
 137 open-source and commercial generators, achieving unprecedented model coverage. However, both
 138 datasets emphasize open repositories rather than real social media distributions, and neither provides
 139 multi-class labels, tampering masks, or explanations. In contrast, **So-Fake** is the first dataset explicitly
 140 targeting **social media forgeries**, with two distinctive advantages: (1) social-media-oriented data col-
 141 lection rather than relying on open repositories or community uploads; and (2) enriched annotations
 142 and benchmarks, including multi-class labels, tampered region masks, explanatory rationales, and a
 143 dedicated OOD split based on real social media data for rigorous cross-domain evaluation. A detailed
 144 comparison with existing image forgery datasets is provided in Table 1.

2.2 IMAGE FORGERY DETECTION, LOCALIZATION, AND EXPLANATION

145 Recent developments in forgery detection have focused primarily on using deep neural networks to
 146 distinguish authentic content from manipulated content. While these methods (Kroiß & Reschke,
 147 2025; Chen et al., 2022; Pei et al., 2024; Wang et al., 2025b) achieve strong performance by capturing
 148 subtle visual artifacts, they often lack robustness when facing novel manipulation types or content
 149 domains. To address these limitations, researchers have increasingly turned to localization approaches
 150 that identify specific tampered regions. Image forgery detection and localization (IFDL) (Dong et al.,
 151 2023; Guo et al., 2024; Guillaro et al., 2023; Zhang et al., 2023; Liu et al., 2022) provides more
 152 granular and interpretable insights than global classification alone, enabling a better understanding
 153 of manipulation techniques. However, current localization datasets focus almost exclusively on
 154 facial forgeries (Wang et al., 2025a; Liang et al., 2024), neglecting the diverse manipulation types
 155 characteristic of social media images. In parallel with addressing data limitations, interpretability has
 156 emerged as a critical frontier, with recent approaches attempting to generate human-understandable
 157 justifications alongside detection. Motivated by recent vision-language models, several works,
 158 such as ForgeryGPT (Li et al., 2024b), SIDA (Huang et al., 2025b), FakeShield (Xu et al., 2024),
 159 FakeScope (Li et al., 2025), and LEGION (Kang et al., 2025) can generate explanations, they typically
 160 require extensive manual annotations and produce superficial descriptions that fail to reveal genuine
 161 model reasoning. In contrast to these approaches, So-Fake-R1 applies reinforcement learning to

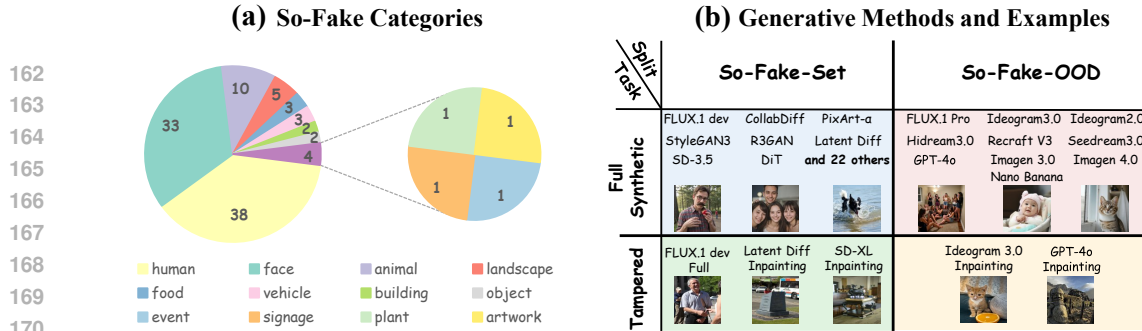


Figure 2: (a) Category distribution of So-Fake across 12 semantic classes. (b) Generative methods and examples for each split-task combination.

enhance the consistency and informativeness of model outputs, enabling detection, localization, and explanation within a unified framework, while reducing reliance on manual annotations.

3 DATASET

3.1 OVERVIEW

Social media platforms host vast volumes of user-generated images that differ substantially from standard academic datasets. Unlike curated benchmarks, these images cover highly diverse and informal content categories (Dell’Anna et al., 2025), often contain compression artifacts or mixed editing traces (Cozzolino et al., 2024; Huang et al., 2025b), and are increasingly interspersed with synthetic media generated by commercial models such as GPT-4o (Hurst et al., 2024), Hidream3.0 (HiDream-ai, 2025), and Imagen4 (Google, 2025a). These factors make forgery detection in social media particularly challenging, as models must generalize across heterogeneous, noisy, and manipulation-rich distributions, highlighting the need for realistic benchmarks. However, collecting and releasing large-scale authentic social media imagery is severely constrained by platform policies and privacy concerns, making it infeasible to construct a fully open benchmark directly from these sources.

To address these challenges, we propose **So-Fake**, a benchmark explicitly designed for social-media-oriented forgery detection. So-Fake consists of two complementary components: (i) **So-Fake-Set**, a controlled in-domain benchmark, and (ii) **So-Fake-OOD**, for cross-domain robustness testing. Both components are built under a unified 12-class taxonomy spanning humans, objects, events, and natural scenes (Figure 2(a)), ensuring broad semantic coverage representative of social media content. Specifically, **So-Fake-Set** combines diverse public datasets with systematically generated forgeries, providing an open and scalable alternative to unreleasable social media data. The complete list of generative models used in So-Fake-Set is provided in Appendix B.1. **So-Fake-OOD** integrates authentic Reddit images with forgeries synthesized by entirely disjoint commercial generative models, thereby introducing realistic distributional shifts for robust generalization testing (Figure 2(b)).

3.2 DATA COLLECTION

So-Fake-Set. We select real images from COCO (Lin et al., 2014), Flickr30k (Plummer et al., 2017), OpenImages (Benenson & Ferrari, 2022) and WIDER (Xiong et al., 2015), as these datasets contain complex scenes with humans, animals, diverse environments, and daily activities typical of social media content. We also incorporate CelebA (Liu et al., 2015), OpenForensics (Le et al., 2021), and FFHQ (Karras et al., 2021b) to ensure comprehensive coverage of facial content, which constitutes a significant portion of social media imagery. In total, So-Fake-Set comprises approximately 650K real images, 650K fully synthetic samples, and 650K tampered samples, as shown in Figure 3(a) (left).

So-Fake-OOD. For the OOD benchmark, we collect images from Reddit via its official API. Reddit provides diverse, informal user-generated content across our 12 predefined categories, but with styles and quality levels that differ markedly from the open datasets used in So-Fake-Set, creating a realistic domain shift (illustrated in Appendix C.1). Importantly, Reddit’s content policy permits non-commercial academic use, ensuring legal compliance (Appendix E). From this collection, we retain around 33K images as real samples, some of which are further used to generate full synthetic and tampered counterparts, resulting in 33K per class. This design enables evaluation under both real image shifts and generative method shifts, as demonstrated in Figure 3(a) (right).

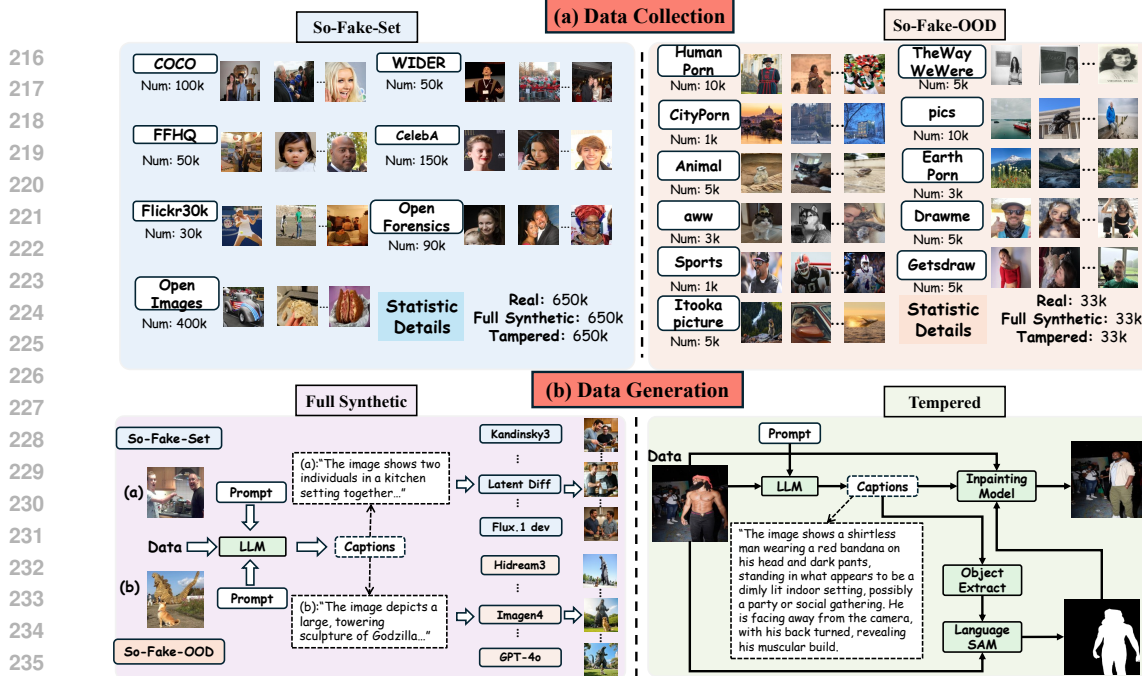


Figure 3: (a) Data collection sources of So-Fake-Set and So-Fake-OOD with representative examples and statistics. (b) Data generation pipelines for full synthetic and tampered images.

3.3 DATA GENERATION

We generate two types of synthetic images: **full synthetic** and **tampered**. Figure 3 (b) illustrates their corresponding generation pipelines, which we detail below.

Full Synthetic Images. To produce full synthetic images, we adopt two main categories of generation techniques: **GAN-based** and **diffusion-based**. For GAN-based methods, we follow the official implementation guidelines provided by the authors. For diffusion-based approaches, we employ a text-to-image generation pipeline, divided into two stages: **(1) Caption Generation.** We evaluated several captioning models for generating text-to-image captions and selected Qwen2.5-VL-7B (Bai et al., 2025) based on experimental results (Appendix B.2). **(2) Image Synthesis.** The generated captions are then fed into different sets of generative models. For So-Fake-Set, we employ 30 architectures spanning both GAN-based and diffusion-based paradigms, selected to maximize architectural diversity and category coverage (see Appendix B.1). For So-Fake-OOD, we instead adopt state-of-the-art commercial generators, including Hidream 3.0 (HiDream-ai, 2025), Nano Banana (Google, 2025b), and Imagen 4 (Google, 2025a), as summarized in Figure 2(b). **(3) Quality Assessment.** Finally, all generated outputs from both GAN-based and diffusion-based methods are subjected to the same quality control process. We combined automated filtering with human evaluation: five expert reviewers assessed generated samples on realism, consistency, and appropriateness using a five-point scale, removing low-quality images after secondary review. This process guarantees that both So-Fake-Set and So-Fake-OOD maintain consistently high quality. Further details are provided in Appendix B.3, with an illustrative example in Figure 7.

Tampered Images. To simulate partial forgeries common in social media imagery, we employ image inpainting techniques that replace specific regions while preserving the rest of the original image. For So-Fake-Set, we use three state-of-the-art inpainting models, including FLUX.1-Fill-dev (Labs, 2024), Latent Diffusion (Rombach et al., 2022), and Stable Diffusion-XL (Podell et al., 2024), chosen for their high visual quality and diversity of generative styles. We first use Qwen2.5-VL-7B (Bai et al., 2025) to generate captions for the source images. An Object Extract module then identifies candidate entities (e.g., “man”) from these captions using a lightweight NLP parser. The extracted object labels are passed to LangSAM (lang-sam team, 2024) to generate precise masks for the corresponding regions. Each inpainting model subsequently receives three inputs—the original image, the extracted mask, and the caption—ensuring semantic consistency between the replaced regions and their surrounding context. For So-Fake-OOD, we adopt the same tampering pipeline as So-Fake-Set but replace the inpainting models with GPT-4o (Hurst et al., 2024), and

270 Ideogram 3.0 (Ideogram, 2025), ensuring evaluation on unseen manipulation techniques. This design
 271 simultaneously introduces distribution shift in real images and manipulation methods, yielding a
 272 more realistic OOD benchmark.

274 4 METHOD

275 4.1 OVERVIEW

276 We introduce **So-Fake-R1** as a unified vision–language policy optimization baseline for
 277 our benchmark. It formulates forgery detection
 278 as a multi-objective reinforcement learning problem,
 279 where Group Relative Policy Optimization (GRPO)
 280 is used to align three complementary
 281 goals: detection, localization, and explanation.
 282 The two-stage pipeline first establishes a stable
 283 reasoning format through cold-start supervised
 284 tuning, and then refines the model with GRPO
 285 to jointly enhance task synergy, as illustrated in Figure 4 (a). This design offers two advantages:
 286 (i) balanced optimization, where gains in one task do not compromise others, and (ii) structured
 287 interpretability guided by rule-based rewards, reducing reliance on additional human supervision.
 288

289 4.2 TRAINING

290 **Stage 1: Cold start.** We fine-tune the base model on a curated set of 9,000 images from So-Fake-Set
 291 (balanced across the three classes, with annotations generated by GPT-4o and subsequently refined
 292 through strict expert review; see Appendix D.2) to align it with our reasoning format and structured
 293 output requirements. This initialization is essential for teaching the model consistent formatting
 294 and multi-granular reasoning, without which reinforcement learning would fail to converge reliably.
 295 The dataset is intentionally kept small to prevent overfitting while still providing a strong prior for
 296 subsequent optimization, reinforced by structured reasoning cues.

297 **Stage 2: GRPO training.** Building on this initialization, we apply GRPO to refine the model
 298 jointly across detection, localization, and explanation. Unlike cold-start stage, which only provides
 299 static supervision, GRPO incorporates rule-based rewards that capture complementary objectives and
 300 encourage balanced improvements across tasks. This stage is particularly critical for harmonizing
 301 reasoning quality with localization precision, while avoiding reliance on manual annotations.

302 As shown in Section 5.5, the two stages provide complementary gains and yield the best overall
 303 performance. Detailed specifications of the cold-start dataset construction, reward weighting strategy,
 304 and training hyperparameter choices are provided in the Appendix D.2.

305 4.3 REWARD FUNCTIONS

306 The reward function is designed to align with the three core outputs of So-Fake-R1: explanation,
 307 detection, and localization. Accordingly, we group the components into three categories, each
 308 providing complementary signals. **(1) Explanation format rewards.** To encourage interpretable
 309 reasoning, we adopt a *format reward* that enforces structured outputs. Specifically, explanations must
 310 appear inside `<think>...</think>` and final answers inside `<answer>...</answer>` tags.
 311 This ensures parseable reasoning traces and stabilizes optimization. **(2) Detection reward.** We assign
 312 a reward based on the correctness of the predicted label (REAL, TAMPERED, FULL_SYNTHETIC),
 313 extracted from the `<answer>` tags. Correct predictions for REAL or FULL SYNTHETIC images
 314 receive a base reward. For TAMPERED images, which typically involve subtle and localized
 315 manipulations and are thus harder to detect, a higher reward is assigned. This weighting prevents
 316 optimization from being biased toward the easier classes and ensures balanced training across all
 317 three categories. **(3) Localization rewards.** For images predicted as TAMPERED, we provide
 318 additional rewards to enforce precise localization: (a) a *format reward* ensures that bounding boxes
 319 follow a strict coordinate specification; (b) an *IoU reward* grants a positive score when predicted
 320 boxes achieve Intersection-over-Union (IoU) > 0.5 with the ground truth; (c) an *L1 reward* further

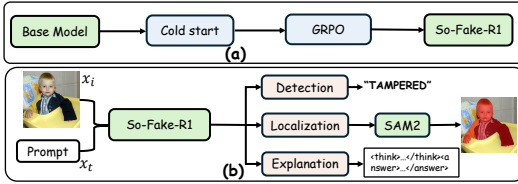


Figure 4: (a) Training pipeline with SFT and GRPO. (b) Inference pipeline producing detection, localization, and explanation outputs.

refines accuracy by rewarding predictions within 10 pixels of the ground truth coordinates. For REAL and FULL_SYNTHETIC images, default values are assigned to maintain balanced gradient signals across all classes. The total reward combines these signals:

$$R_{\text{total}} = \lambda_{\text{fmt}} R_{\text{fmt}} + \lambda_{\text{cls}} R_{\text{cls}} + \lambda_{\text{seg.fmt}} R_{\text{seg.fmt}} + \lambda_{\text{IoU}} R_{\text{IoU}} + \lambda_{\text{L1}} R_{\text{L1}}, \quad (1)$$

where λ controls the relative weight of each component. This decomposition ensures that So-Fake-R1 is jointly optimized for structured reasoning, reliable detection, and fine-grained localization. The exact reward weights, scoring criteria, and implementation details are reported in the Appendix D.1.

4.4 INFERENCE PROCEDURE

At inference time, So-Fake-R1 takes as input an image x_i together with a task prompt x_t and produces three complementary outputs, as illustrated in Figure 4(b). **Explanation:** a hierarchical reasoning trace enclosed in `<think>...</think>`, which analyzes the image at different perspectives before reaching a conclusion. **Detection:** a class label (REAL, TAMPERED, or FULL_SYNTHETIC) reported within `<answer>...</answer>` tags. **Localization:** for tampered cases, So-Fake-R1 outputs bounding-box coordinates in the format `<|box_start|>(x1, y1, x2, y2)<|box_end|>`. These coarse boxes are then passed to SAM2 (Ravi et al., 2024), which refines the bounding boxes into dense segmentation masks.

5 EXPERIMENT

5.1 EXPERIMENTAL SETTINGS

Methods. For a fair and comprehensive comparison of So-Fake-R1 across detection, localization, and explanation tasks, we evaluate against three representative groups of baselines: (1) **Detection-only methods.** CnnSpot (Frank & Holz, 2021), UnivFD (Ojha et al., 2023), FreAware (Tan et al., 2024b), and NPR (Tan et al., 2024a). (2) **Image Forgery Detection and Localization (IFDL) methods.** HIFI-Net (Guo et al., 2024), TruFor (Guillaro et al., 2023), PSCC-Net (Liu et al., 2022), SIDA (Huang et al., 2025b), and FakeShield (Xu et al., 2024). (3) **Explanation-oriented methods.** LLaVA-1.5-13B (Liu et al., 2023), LISA (Lai et al., 2024), InternVL3-8B (Zhu et al., 2025), Qwen2.5-VL-7B (Bai et al., 2025), and DeepSeek-VL-7B (DeepSeek-AI et al., 2025). Unless otherwise noted, all baselines are fine-tuned on the So-Fake-Training Set. Exceptions include: FakeShield, which requires paired image-text inputs and is evaluated using its publicly released checkpoints; and HIFI-Net, which is evaluated using its pre-trained weights due to the unavailability of complete training code.

Metrics. We evaluate models across the three tasks defined by So-Fake. For **detection**, we report image-level accuracy (Acc) and F1. For **localization**, we adopt Intersection over Union (IoU) and mask-level F1, which capture the ability to pinpoint subtle local edits that are prevalent in social-media manipulations. For **explanation**, we employ two complementary metrics: (1) Cosine Semantic Similarity (CSS), which captures semantic alignment between embeddings of predicted and ground-truth explanations, and (2) ROUGE-L, which quantifies textual overlap through longest common subsequence matching. Ground-truth explanations were first generated with Claude Opus 4.1 (light logo, 2025), then carefully revised and validated by human experts. In total, over 3,000 high-quality explanations were curated, providing reliable supervision for quantitative benchmarking.

5.2 COMPARISON RESULTS ON SO-FAKE-SET

As shown in Table 2, our method achieves superior performance across all metrics, surpassing the second-best method by **1.3%** in detection accuracy, **1.1%** in localization IoU, and significantly higher CSS scores for explanation quality. These results demonstrate the effectiveness of So-Fake-R1.

5.3 COMPARISON RESULTS ON SO-FAKE-OOD

For fairness, we evaluate both the *zero-shot* and *fine-tune* settings, where models are fine-tuned on the training split of So-Fake-Set and evaluated on So-Fake-OOD. As shown in Table 3, So-Fake-R1 achieves the highest performance across all metrics, demonstrating superior cross-domain generalization compared to other methods.

Table 2: Performance comparison on So-Fake-Set. Methods marked with “*” denote results obtained using publicly released weights without fine-tuning.

Method	Year	Type	Detection		Localization		Explanation	
			Acc	FI	IOU	FI	ROUGE-L	CSS
CnnSpot	2021	Detection	89.6	87.7	-	-	-	-
UnivFD	2023	Detection	84.0	63.8	-	-	-	-
FreAware	2024	Detection	85.6	73.1	-	-	-	-
NPR	2024	Detection	81.8	61.5	-	-	-	-
HIFI-Net*	2022	IFDL	39.0	25.2	12.1	18.3	-	-
TruFor	2023	IFDL	87.3	85.9	47.5	57.6	-	-
PSCC-Net	2022	IFDL	84.2	81.1	46.3	54.8	-	-
FakeShield*	2024	IFDL	67.0	64.1	33.7	46.1	0.2412	0.5143
SIDA	2025	IFDL	91.9	91.5	44.1	58.9	0.4313	0.7987
LLaVA-1.5-13B	2024	LLM	83.5	82.9	29.8	38.1	0.4213	0.7877
LISA	2024	LLM	87.4	85.9	40.5	47.6	0.4246	0.7861
DeepSeek-VL-7B	2025	LLM	83.7	81.1	27.8	35.4	0.4376	0.8196
Qwen2.5-VL-7B	2024	LLM	91.2	90.8	42.7	50.1	0.4515	0.8411
InternVL3-8B	2025	LLM	87.6	87.3	41.1	48.5	0.4553	0.8341
Ours	2025	LLM	93.2	92.9	48.6	63.9	0.4718	0.8769

Table 3: Performance comparison on So-Fake-OOD with both *zero-shot* and *fine-tune* settings.

Method	Detection				Localization				Explanation			
	zero shot		fine tune		zero shot		fine tune		zero shot		fine tune	
	Acc	FI	Acc	FI	IOU	FI	IOU	FI	ROUGE-L	CSS	ROUGE-L	CSS
CnnSpot	32.8	29.7	65.2	63.8	-	-	-	-	-	-	-	-
UnivFD	45.3	43.7	63.3	40.2	-	-	-	-	-	-	-	-
FreAware	52.3	48.3	56.5	54.6	-	-	-	-	-	-	-	-
NPR	55.6	47.1	57.6	50.9	-	-	-	-	-	-	-	-
HIFI-Net*	54.3	47.3	-	-	15.2	22.4	-	-	-	-	-	-
TruFor	44.7	12.6	55.9	53.1	7.8	11.2	32.3	41.1	-	-	-	-
PSCC-Net	35.4	9.9	48.9	46.1	20.5	30.7	41.1	48.7	-	-	-	-
FakeShield*	42.1	35.7	-	-	24.9	30.2	-	-	0.2561	0.5214	-	-
SIDA	50.1	49.8	73.1	72.2	25.4	38.9	40.1	49.3	0.1724	0.4026	0.4135	0.7899
LLaVA-1.5-13B	34.1	33.2	70.9	70.5	9.7	13.8	26.7	35.1	0.1026	0.3321	0.4212	0.7689
LISA	37.6	37.1	70.1	70.0	18.3	21.4	38.2	47.5	0.1663	0.4106	0.4115	0.7881
DeepSeek-VL-7B	35.9	34.0	71.1	70.4	10.3	14.1	25.4	34.6	0.1054	0.3422	0.4212	0.7776
Qwen2.5-VL-7B	38.4	35.7	73.3	72.5	17.5	20.3	42.2	49.9	0.2692	0.5342	0.4371	0.8124
InternVL3-8B	39.1	33.6	71.2	70.1	10.2	13.8	40.4	47.1	0.2653	0.5473	0.4463	0.8231
Ours	-	-	76.4	75.3	-	-	47.8	59.1	-	-	0.4695	0.8421

5.4 EXTERNAL EXPERIMENTS

Robustness Evaluation. We evaluate So-Fake-R1’s robustness against common social media perturbations, including JPEG compression (quality 70/80), resizing (scale 0.5/0.75), and Gaussian noise (variance 5/10). As shown in Table 4, our model maintains strong performance across all degradation scenarios, demonstrating its practical applicability for real-world deployment.

Evaluation on External Social Media Benchmark. To further assess generalization capabilities, we evaluate So-Fake-R1 on SID-Set (Huang et al., 2025b). As shown in Table 5, So-Fake-R1 demonstrates strong cross-dataset generalization after fine-tuning.

Cross-Domain Generalization Analysis. We analyze the generalization capabilities across different generators to understand the challenges posed by So-Fake. As shown in Figure 5, detectors generalize reasonably within So-Fake-Set when training and testing generators share architectural traits, but performance drops sharply across distinct paradigms. In particular, cross-family transfer between GAN and diffusion models is noticeably weaker, and this gap becomes far more pronounced under So-Fake-OOD. This suggests that current detection methods may be overfitting to generator-specific artifacts rather than learning fundamental patterns. Additional analysis is provided in Appendix C.

5.5 ABLATION STUDY

Training Strategy. We evaluate the effectiveness of our two-stage training pipeline. As shown in Table 6, both the cold-start SFT stage and GRPO refinement contribute to final performance. The cold-start stage is crucial for establishing basic detection capabilities, while GRPO significantly improves all metrics. Without cold-start training, the model struggles to properly identify tampered content categories, demonstrating that GRPO alone is insufficient for our challenging detection tasks.

432
433 Table 4: Performance of So-Fake-R1 under different perturbations.
434

	Detection		Localization		Explanation	
	ACC	F1	F1	IOU	ROUGE-L	CSS
JPEG 70	91.5	91.2	60.3	45.1	0.4523	0.8612
JPEG 80	92.0	91.8	61.7	46.3	0.4611	0.8658
Resize 0.5	89.7	89.1	58.4	42.9	0.4352	0.8483
Resize 0.75	90.9	90.3	59.8	44.2	0.4477	0.8540
Gaussian 10	88.3	87.5	54.7	40.5	0.4124	0.8306
Gaussian 5	89.8	89.0	56.1	41.7	0.4239	0.8407
Original	93.2	92.9	63.9	48.6	0.4718	0.8769

442
443 Table 6: Training strategy.
444

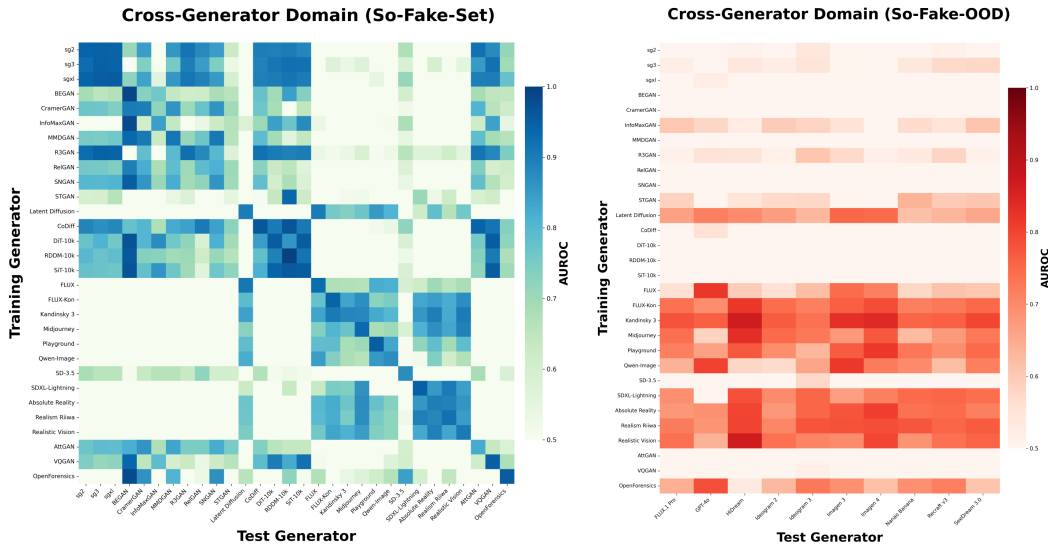
Cold Start	GRPO	Detection Acc.
	✓	63.7
✓		89.3
✓	✓	93.2

445 Table 7: Reward function.
446

	R_{cls}	R_{fmt}	$R_{seg,fmt}$	R_{IOU}	R_{L1}	Acc	IOU
✓						93.1	-
✓	✓	✓		✓		93.1	-
✓	✓	✓	✓	✓	✓	92.9	-
✓	✓	✓	✓	✓	✓	93.2	46.7
✓	✓	✓	✓	✓	✓	93.2	48.6

447 Table 8: Policy model.
448

Policy Model	Detection	
	Acc	F1
InternVL3-8B	91.3	90.8
DeepSeek-VL-7B	88.6	88.1
Qwen2.5-VL-7B	93.2	92.9

469 Figure 5: Cross-generator domain generalization matrix using CNNSpot. Rows indicate training
470 generators and columns indicate test generators, with So-Fake-Set (left) and So-Fake-OOD (right).
471472 **Selection of Reward Functions.** We analyze the impact of different reward function combinations
473 on model performance. As shown in Table 7, using all five reward functions yields the best results.
474475 **Policy Model Selection.** We evaluate several policy models, and Table 8 shows that Qwen2.5-VL-7B
476 achieves the best performance, supporting our final choice.
477478

6 CONCLUSION AND LIMITATION

479480 **Conclusion.** We present **So-Fake**, a benchmark for social-media forgery detection that includes
481 **So-Fake-Set** for training/validation and **So-Fake-OOD** for cross-domain evaluation. We further
482 propose **So-Fake-R1**, an RL-based framework that unifies detection, localization, and explanation,
483 offering a strong baseline in both in-domain and OOD settings. **Limitations.** While So-Fake advances
484 the scale and diversity of forgery benchmarks, it still cannot fully capture the breadth of real-world
485 social media content or the rapidly evolving landscape of generative models. So-Fake-R1, though
486 effective, remains computationally demanding and may produce inaccurate localization in challenging
487 cases, as shown in Appendix D.4. Finally, our benchmark focuses on still images, leaving video and
488 multimodal forgeries as important directions for future work.
489

486 **Ethics Statement.** This work adheres to ethical research practices detailed throughout our paper.
 487 Data collection from Reddit follows their public content policy for non-commercial academic use
 488 (Appendix E), with multi-stage human review processes to filter inappropriate content (Appendix B.3).
 489 Our research aims to advance detection capabilities against malicious synthetic media, with datasets
 490 and models released exclusively for academic research under controlled access. We acknowledge the
 491 dual-use nature of generative AI research and commit to responsible disclosure practices to minimize
 492 potential misuse while maximizing societal benefits through improved detection capabilities.

493 **Reproducibility Statement.** We provide comprehensive implementation details to ensure full
 494 reproducibility. Complete dataset construction pipelines are detailed in Section 3 and Appendix B,
 495 including all 40 generative methods (Table 9), human evaluation protocols (Section B.3), and
 496 quality control procedures (Figure 6). Training configurations, hyperparameters, and reward function
 497 specifications for So-Fake-R1 are provided in Appendix D.1. Baseline implementations follow official
 498 guidelines where available, with detailed configurations in Section D.2. We commit to releasing
 499 the So-Fake dataset, So-Fake-R1 source code, trained model weights, and evaluation protocols to
 500 facilitate future research and enable direct comparison with our results.

501 **LLM Usage Statement.** We declare that large language models (LLMs) were used exclusively
 502 for language editing and stylistic improvements in this manuscript. They did not contribute to the
 503 conceptual, methodological, or experimental aspects of the work.

505 REFERENCES

507 Vladimir Arkhipkin, Andrei Filatov, Viacheslav Vasilev, Anastasia Maltseva, Said Azizov, Igor
 508 Pavlov, Julia Agafonova, Andrey Kuznetsov, and Denis Dimitrov. Kandinsky 3.0 technical report,
 509 2023.

510 Shuai Bai, Keqin Chen, Xuejing Liu, Jialin Wang, Wenbin Ge, Sibo Song, Kai Dang, Peng Wang,
 511 Shijie Wang, Jun Tang, Humen Zhong, Yuanzhi Zhu, Ming-Hsuan Yang, Zhaohai Li, Jianqiang
 512 Wan, Pengfei Wang, Wei Ding, Zheren Fu, Yiheng Xu, Jiabo Ye, Xi Zhang, Tianbao Xie, Zesen
 513 Cheng, Hang Zhang, Zhibo Yang, Haiyang Xu, and Junyang Lin. Qwen2.5-v1 technical report.
 514 *Arxiv*, 2025.

515 Jason Baldridge, Jakob Bauer, Mukul Bhutani, Nicole Brichtova, Andrew Bunner, Kelvin Chan,
 516 Yichang Chen, Sander Dieleman, Yuqing Du, Zach Eaton-Rosen, Hongliang Fei, Nando de Fre-
 517 itas, Yilin Gao, Evgeny Gladchenko, Sergio Gómez Colmenarejo, Mandy Guo, Alex Haig, Will
 518 Hawkins, Hexiang Hu, Huilian Huang, Tobenna Peter Igwe, Christos Kaplanis, Siavash Kho-
 519 dadadeh, Yelin Kim, Ksenia Konyushkova, Karol Langner, Eric Lau, Shixin Luo, Sona Mokrá,
 520 Henna Nandwani, Yasumasa Onoe, Aäron van den Oord, Zarana Parekh, Jordi Pont-Tuset, Hang
 521 Qi, Rui Qian, Deepak Ramachandran, Poorva Rane, Abdullah Rashwan, Ali Razavi, Robert Riachi,
 522 Hansa Srinivasan, Srivatsan Srinivasan, Robin Strudel, Benigno Uria, Oliver Wang, Su Wang,
 523 Austin Waters, Chris Wolff, Auriel Wright, Zhisheng Xiao, Hao Xiong, Keyang Xu, Marc van Zee,
 524 Junlin Zhang, Katie Zhang, Wenlei Zhou, Konrad Zolna, Ola Aboubakar, Canfer Akbulut, Oscar
 525 Akerlund, Isabela Albuquerque, Nina Anderson, Marco Andreetto, Lora Aroyo, Ben Bariach,
 526 David Barker, Sherry Ben, Dana Berman, Courtney Biles, Irina Blok, Pankil Botadra, Jenny Bren-
 527 nan, Karla Brown, John Buckley, Rudy Bunel, Elie Bursztein, Christina Butterfield, Ben Caine,
 528 Viral Carpenter, Norman Casagrande, Ming-Wei Chang, Solomon Chang, Shamik Chaudhuri, Tony
 529 Chen, John Choi, Dmitry Churbanau, Nathan Clement, Matan Cohen, Forrester Cole, Mikhail
 530 Dektiarev, Vincent Du, Praneet Dutta, Tom Eccles, Ndidi Elue, Ashley Feden, Shlomi Fruchter,
 531 Frankie Garcia, and Roopal Garg. Imagen 3. *Arxiv*, 2024.

532 Marc G. Bellemare, Ivo Danihelka, Will Dabney, Shakir Mohamed, Balaji Lakshminarayanan,
 533 Stephan Hoyer, and Rémi Munos. The cramer distance as a solution to biased wasserstein
 534 gradients. *Arxiv*, 2017.

536 Rodrigo Benenson and Vittorio Ferrari. From colouring-in to pointillism: revisiting semantic
 537 segmentation supervision. *Arxiv*, 2022.

538 David Berthelot, Tom Schumm, and Luke Metz. BEGAN: boundary equilibrium generative adver-
 539 sar-
 ial networks. *Arxiv*, 2017.

540 Chaitali Bhattacharyya, Hanxiao Wang, Feng Zhang, Sungho Kim, and Xiatian Zhu. Diffusion
 541 deepfake. *Arxiv*, 2024.

542

543 Liang Chen, Yong Zhang, Yibing Song, Lingqiao Liu, and Jue Wang. Self-supervised learning of
 544 adversarial example: Towards good generalizations for deepfake detection. In *CVPR*, 2022.

545 Riccardo Corvi, Davide Cozzolino, Giada Zingarini, Giovanni Poggi, Koki Nagano, and Luisa
 546 Verdoliva. On the detection of synthetic images generated by diffusion models. In *ICASSP*, 2023.

547

548 Davide Cozzolino, Giovanni Poggi, Riccardo Corvi, Matthias Nießner, and Luisa Verdoliva. Raising
 549 the bar of ai-generated image detection with CLIP. In *CVPR*, 2024.

550

551 Hao Dang, Feng Liu, Joel Stehouwer, Xiaoming Liu, and Anil K. Jain. On the detection of digital
 552 face manipulation. In *CVPR*, 2020.

553

554 DeepSeek-AI, Daya Guo, Dejian Yang, Haowei Zhang, Junxiao Song, Ruoyu Zhang, Runxin Xu,
 555 Qihao Zhu, Shirong Ma, Peiyi Wang, Xiao Bi, Xiaokang Zhang, Xingkai Yu, Yu Wu, Z. F. Wu,
 556 Zhibin Gou, Zhihong Shao, Zhuoshu Li, Ziyi Gao, Aixin Liu, Bing Xue, Bingxuan Wang, Bochao
 557 Wu, Bei Feng, Chengda Lu, Chenggang Zhao, Chengqi Deng, Chenyu Zhang, Chong Ruan,
 558 Damai Dai, Deli Chen, Dongjie Ji, Erhang Li, Fangyun Lin, Fucong Dai, Fuli Luo, Guangbo Hao,
 559 Guanting Chen, Guowei Li, H. Zhang, Han Bao, Hanwei Xu, Haocheng Wang, Honghui Ding,
 560 Huajian Xin, Huazuo Gao, Hui Qu, Hui Li, Jianzhong Guo, Jiashi Li, Jiawei Wang, Jingchang
 561 Chen, Jingyang Yuan, Junjie Qiu, Junlong Li, J. L. Cai, Jiaqi Ni, Jian Liang, Jin Chen, Kai Dong,
 562 Kai Hu, Kaige Gao, Kang Guan, Kexin Huang, Kuai Yu, Lean Wang, Lecong Zhang, Liang Zhao,
 563 Litong Wang, Liyue Zhang, Lei Xu, Leyi Xia, Mingchuan Zhang, Minghua Zhang, Minghui Tang,
 564 Meng Li, Miaojun Wang, Mingming Li, Ning Tian, Panpan Huang, Peng Zhang, Qiancheng Wang,
 565 Qinyu Chen, Qiushi Du, Ruiqi Ge, Ruisong Zhang, Ruizhe Pan, Runji Wang, R. J. Chen, R. L.
 566 Jin, Ruyi Chen, Shanghao Lu, Shangyan Zhou, Shanhuang Chen, Shengfeng Ye, Shiyu Wang,
 567 Shuiping Yu, Shunfeng Zhou, Shuting Pan, and S. S. Li. Deepseek-r1: Incentivizing reasoning
 568 capability in llms via reinforcement learning. *Arxiv*, 2025.

569

570 Stefano Dell’Anna, Andrea Montibeller, and Giulia Boato. Truefake: A real world case dataset of
 571 last generation fake images also shared on social networks, 2025.

572

573 Chengbo Dong, Xinru Chen, Ruohan Hu, Juan Cao, and Xirong Li. Mvss-net: Multi-view multi-scale
 574 supervised networks for image manipulation detection. *PAMI*, 2023.

575

576 Patrick Esser, Sumith Kulal, Andreas Blattmann, Rahim Entezari, Jonas Müller, Harry Saini, Yam
 577 Levi, Dominik Lorenz, Axel Sauer, Frederic Boesel, Dustin Podell, Tim Dockhorn, Zion English,
 578 and Robin Rombach. Scaling rectified flow transformers for high-resolution image synthesis. In
 579 *ICML*, 2024.

580

581 Joel Frank and Thorsten Holz. [RE] cnn-generated images are surprisingly easy to spot...for now.
 582 *Arxiv*, 2021.

583

584 Yu Gao, Lixue Gong, Qiushan Guo, Xiaoxia Hou, Zhichao Lai, Fanshi Li, Liang Li, Xiaochen Lian,
 585 Chao Liao, Liyang Liu, Wei Liu, Yichun Shi, Shiqi Sun, Yu Tian, Zhi Tian, Peng Wang, Rui Wang,
 586 Xuanda Wang, Xun Wang, Ye Wang, Guofeng Wu, Jie Wu, Xin Xia, Xuefeng Xiao, Zhonghua
 587 Zhai, Xinyu Zhang, Qi Zhang, Yuwei Zhang, Shijia Zhao, Jianchao Yang, and Weilin Huang.
 588 Seedream 3.0 technical report. *Arxiv*, 2025.

589

590 Google. Imagen4.0. <https://deepmind.google/models/imagen/>, 2025a.

591

592 Google. Nanobanana. <https://aistudio.google.com/models/gemini-2-5-flash-image>, 2025b.

593

594 Fabrizio Guillaro, Davide Cozzolino, Avneesh Sud, Nicholas Dufour, and Luisa Verdoliva. Trufor:
 595 Leveraging all-round clues for trustworthy image forgery detection and localization. In *CVPR*,
 596 2023.

597

598 Xiao Guo, Xiaohong Liu, Zhiyuan Ren, Steven Grosz, Iacopo Masi, and Xiaoming Liu. Hierarchical
 599 fine-grained image forgery detection and localization. In *CVPR*, 2023.

594 Xiao Guo, Xiaohong Liu, Iacopo Masi, and Xiaoming Liu. Language-guided hierarchical fine-grained
 595 image forgery detection and localization. *Arxiv*, 2024.

596

597 Yinan He, Bei Gan, Siyu Chen, Yichun Zhou, Guojun Yin, Luchuan Song, Lu Sheng, Jing Shao,
 598 and Ziwei Liu. Forgerynet: A versatile benchmark for comprehensive forgery analysis. In *CVPR*,
 599 2021.

600 Zhenliang He, Wangmeng Zuo, Meina Kan, Shiguang Shan, and Xilin Chen. Arbitrary facial attribute
 601 editing: Only change what you want. *PAMI*, 2017.

602

603 HiDream-ai. Hidream-11. <https://github.com/HiDream-ai/HiDream-11>, 2025.

604

605 Yan Hong, Jianming Feng, Haoxing Chen, Jun Lan, Huijia Zhu, Weiqiang Wang, and Jianfu Zhang.
 606 Wildfake: A large-scale and hierarchical dataset for ai-generated images detection. In Toby Walsh,
 607 Julie Shah, and Zico Kolter (eds.), *AAAI*, 2025.

608 Edward J. Hu, Yelong Shen, Phillip Wallis, Zeyuan Allen-Zhu, Yuanzhi Li, Shean Wang, and Weizhu
 609 Chen. Lora: Low-rank adaptation of large language models. *Arxiv*, 2021.

610

611 Yuqi Hu, Longguang Wang, Xian Liu, Ling-Hao Chen, Yuwei Guo, Yukai Shi, Ce Liu, Anyi Rao,
 612 Zeyu Wang, and Hui Xiong. Simulating the real world: A unified survey of multimodal generative
 613 models. *Arxiv*, 2025.

614 Nick Huang, Aaron Gokaslan, Volodymyr Kuleshov, and James Tompkin. The GAN is dead; long
 615 live the gan! A modern GAN baseline. In Amir Globersons, Lester Mackey, Danielle Belgrave,
 616 Angela Fan, Ulrich Paquet, Jakub M. Tomczak, and Cheng Zhang (eds.), *NeurIPS*, 2024a.

617

618 Wenxuan Huang, Bohan Jia, Zijie Zhai, Shaosheng Cao, Zheyu Ye, Fei Zhao, Zhe Xu, Yao Hu, and
 619 Shaohui Lin. Vision-r1: Incentivizing reasoning capability in multimodal large language models.
 620 *arXiv preprint arXiv:2503.06749*, 2025a.

621 Zhengchao Huang, Bin Xia, Zicheng Lin, Zhun Mou, and Wenming Yang. FFAA: multimodal large
 622 language model based explainable open-world face forgery analysis assistant. *Arxiv*, 2024b.

623

624 Zhenglin Huang, Jinwei Hu, Xiangtai Li, Yiwei He, Xingyu Zhao, Bei Peng, Baoyuan Wu, Xiaowei
 625 Huang, and Guangliang Cheng. SIDA: social media image deepfake detection, localization and
 626 explanation with large multimodal model. *CVPR*, 2025b.

627 Ziqi Huang, Kelvin C. K. Chan, Yuming Jiang, and Ziwei Liu. Collaborative diffusion for multi-modal
 628 face generation and editing. In *CVPR*, 2023.

629

630 Aaron Hurst, Adam Lerer, Adam P. Goucher, Adam Perelman, Aditya Ramesh, Aidan Clark, AJ Os-
 631 trow, Akila Welihinda, Alan Hayes, Alec Radford, Aleksander Madry, Alex Baker-Whitcomb, Alex
 632 Beutel, Alex Borzunov, Alex Carney, Alex Chow, Alex Kirillov, Alex Nichol, Alex Paino, Alex
 633 Renzin, Alex Tachard Passos, Alexander Kirillov, Alexi Christakis, Alexis Conneau, Ali Kamali,
 634 Allan Jabri, Allison Moyer, Allison Tam, Amadou Crookes, Amin Tootoonchian, Ananya Kumar,
 635 Andrea Vallone, Andrej Karpathy, Andrew Braunstein, Andrew Cann, Andrew Codispoti, Andrew
 636 Galu, Andrew Kondrich, Andrew Tulloch, Andrey Mishchenko, Angela Baek, Angela Jiang, An-
 637 toine Pelisse, Antonia Woodford, Anuj Gosalia, Arka Dhar, Ashley Pantuliano, Avi Nayak, Avital
 638 Oliver, Barret Zoph, Behrooz Ghorbani, Ben Leimberger, Ben Rossen, Ben Sokolowsky, Ben
 639 Wang, Benjamin Zweig, Beth Hoover, Blake Samic, Bob McGrew, Bobby Spero, Bogo Giertler,
 640 Bowen Cheng, Brad Lightcap, Brandon Walkin, Brendan Quinn, Brian Guarraci, Brian Hsu, Bright
 641 Kellogg, Brydon Eastman, Camillo Lugaresi, Carroll L. Wainwright, Cary Bassin, Cary Hudson,
 642 Casey Chu, Chad Nelson, Chak Li, Chan Jun Shern, Channing Conger, Charlotte Barette, Chelsea
 643 Voss, Chen Ding, Cheng Lu, Chong Zhang, Chris Beaumont, Chris Hallacy, Chris Koch, Christian
 644 Gibson, Christina Kim, Christine Choi, Christine McLeavey, Christopher Hesse, Claudia Fischer,
 645 Clemens Winter, Coley Czarnecki, Colin Jarvis, Colin Wei, Constantin Koumouzelis, and Dane
 646 Sherburn. Gpt-4o system card. *Arxiv*, 2024.

647

Ideogram. Ideogram2.0. <https://about.ideogram.ai/2.0>, 2024.

Ideogram. Ideogram3.0. <https://about.ideogram.ai/3.0>, 2025.

648 Yikun Ji, Hong Yan, Jun Lan, Huijia Zhu, Weiqiang Wang, Qi Fan, Liqing Zhang, and Jianfu Zhang.
 649 Interpretable and reliable detection of ai-generated images via grounded reasoning in mllms. *Arxiv*,
 650 2025.

651 Hengrui Kang, Siwei Wen, Zichen Wen, Junyan Ye, Weijia Li, Peilin Feng, Baichuan Zhou, Bin
 652 Wang, Dahua Lin, Linfeng Zhang, and Conghui He. LEGION: learning to ground and explain for
 653 synthetic image detection. *Arxiv*, 2025.

654 Tero Karras, Samuli Laine, Miika Aittala, Janne Hellsten, Jaakko Lehtinen, and Timo Aila. Analyzing
 655 and improving the image quality of stylegan. In *CVPR*, 2020.

656 Tero Karras, Miika Aittala, Samuli Laine, Erik Härkönen, Janne Hellsten, Jaakko Lehtinen, and Timo
 657 Aila. Alias-free generative adversarial networks. In *NeurIPS*, 2021a.

658 Tero Karras, Samuli Laine, and Timo Aila. A style-based generator architecture for generative
 659 adversarial networks. *PAMI*, 2021b.

660 Lukas Kroiß and Johannes Reschke. Deepfake detection of face images based on a convolutional
 661 neural network. *Arxiv*, 2025.

662 Black Forest Labs. Flux. <https://github.com/black-forest-labs/flux>, 2024.

663 Black Forest Labs. Flux. <https://replicate.com/black-forest-labs/flux-1.1-pro>, 2025.

664 Xin Lai, Zhuotao Tian, Yukang Chen, Yanwei Li, Yuhui Yuan, Shu Liu, and Jiaya Jia. LISA:
 665 reasoning segmentation via large language model. In *CVPR*, 2024.

666 lang-sam team. Lang-segment-anything, 2024. URL <https://github.com/lucamedeiros/lang-segment-anything>.

667 Trung-Nghia Le, Huy H. Nguyen, Junichi Yamagishi, and Isao Echizen. Openforensics: Large-scale
 668 challenging dataset for multi-face forgery detection and segmentation in-the-wild. In *ICCV*, 2021.

669 Kwot Sin Lee, Ngoc-Trung Tran, and Ngai-Man Cheung. Infomax-gan: Improved adversarial image
 670 generation via information maximization and contrastive learning. In *WACV*, 2021.

671 Chun-Liang Li, Wei-Cheng Chang, Yu Cheng, Yiming Yang, and Barnabás Póczos. MMD GAN:
 672 towards deeper understanding of moment matching network. In Isabelle Guyon, Ulrike von
 673 Luxburg, Samy Bengio, Hanna M. Wallach, Rob Fergus, S. V. N. Vishwanathan, and Roman
 674 Garnett (eds.), *NeurIPS*, 2017.

675 Daiqing Li, Aleks Kamko, Ehsan Akhgari, Ali Sabet, Linmiao Xu, and Suhail Doshi. Playground
 676 v2.5: Three insights towards enhancing aesthetic quality in text-to-image generation. *Arxiv*, 2024a.

677 Jiawei Li, Fanrui Zhang, Jiaying Zhu, Esther Sun, Qiang Zhang, and Zheng-Jun Zha. Forgerygpt:
 678 Multimodal large language model for explainable image forgery detection and localization. *Arxiv*,
 679 2024b.

680 Yixuan Li, Yu Tian, Yipo Huang, Wei Lu, Shiqi Wang, Weisi Lin, and Anderson Rocha. Fakescope:
 681 Large multimodal expert model for transparent ai-generated image forensics. *Arxiv*, 2025.

682 Jiawei Liang, Siyuan Liang, Aishan Liu, Xiaojun Jia, Junhao Kuang, and Xiaochun Cao. Poisoned
 683 forgery face: Towards backdoor attacks on face forgery detection. In *ICLR*, 2024.

684 light logo. Claude. <https://claude.ai/>, 2025.

685 Tsung-Yi Lin, Michael Maire, Serge J. Belongie, James Hays, Pietro Perona, Deva Ramanan, Piotr
 686 Dollár, and C. Lawrence Zitnick. Microsoft COCO: common objects in context. In David J. Fleet,
 687 Tomás Pajdla, Bernt Schiele, and Tinne Tuytelaars (eds.), *ECCV*, 2014.

688 Haotian Liu, Chunyuan Li, Qingyang Wu, and Yong Jae Lee. Visual instruction tuning. In *NeurIPS*,
 689 2023.

702 Jiawei Liu, Qiang Wang, Huijie Fan, Yinong Wang, Yandong Tang, and Liangqiong Qu. Residual
 703 denoising diffusion models. In *CVPR*, 2024.

704

705 Ming Liu, Yukang Ding, Min Xia, Xiao Liu, Errui Ding, Wangmeng Zuo, and Shilei Wen. STGAN:
 706 A unified selective transfer network for arbitrary image attribute editing. In *CVPR*, 2019.

707

708 Xiaohong Liu, Yaojie Liu, Jun Chen, and Xiaoming Liu. Pscc-net: Progressive spatio-channel
 709 correlation network for image manipulation detection and localization. *IEEE TCSVT*, 2022.

710

711 Yuqi Liu, Bohao Peng, Zhisheng Zhong, Zihao Yue, Fanbin Lu, Bei Yu, and Jiaya Jia. Seg-zero:
 712 Reasoning-chain guided segmentation via cognitive reinforcement. *Arxiv*, 2025a.

713

714 Ziwei Liu, Ping Luo, Xiaogang Wang, and Xiaoou Tang. Deep learning face attributes in the wild. In
 715 *ICCV*, 2015.

716

717 Ziyu Liu, Zeyi Sun, Yuhang Zang, Xiaoyi Dong, Yuhang Cao, Haodong Duan, Dahua Lin, and Jiaqi
 718 Wang. Visual-rft: Visual reinforcement fine-tuning. *Arxiv*, 2025b.

719

720 Lykon. Absolutereality, 2023. URL <https://huggingface.co/Lykon/AbsoluteReality>.

721

722 Nanye Ma, Mark Goldstein, Michael S. Albergo, Nicholas M. Boffi, Eric Vanden-Eijnden, and
 723 Saining Xie. Sit: Exploring flow and diffusion-based generative models with scalable interpolant
 724 transformers. In Ales Leonardis, Elisa Ricci, Stefan Roth, Olga Russakovsky, Torsten Sattler, and
 725 Gü̈l Varol (eds.), *ECCV*, 2024.

726

727 Midjourney. Midjourney. <https://www.midjourney.com/home>, 2023.

728

729 Takeru Miyato, Toshiki Kataoka, Masanori Koyama, and Yuichi Yoshida. Spectral normalization for
 730 generative adversarial networks. In *ICLR*, 2018.

731

732 Weili Nie, Nina Narodytska, and Ankit Patel. Relgan: Relational generative adversarial networks for
 733 text generation. In *ICLR*, 2019.

734

735 Utkarsh Ojha, Yuheng Li, and Yong Jae Lee. Towards universal fake image detectors that generalize
 736 across generative models. In *CVPR*, 2023.

737

738 OpenAI. GPT-4 technical report. *Arxiv*, 2023.

739

740 Jeongsoo Park and Andrew Owens. Community forensics: Using thousands of generators to train
 741 fake image detectors. In *CVPR*, 2025.

742

743 William Peebles and Saining Xie. Scalable diffusion models with transformers. In *ICCV*, 2023.

744

745 Gan Pei, Jiangning Zhang, Menghan Hu, Guangtao Zhai, Chengjie Wang, Zhenyu Zhang, Jian Yang,
 746 Chunhua Shen, and Dacheng Tao. Deepfake generation and detection: A benchmark and survey.
 747 *Arxiv*, 2024.

748

749 Jiawei Peng, Ju He, Prakhar Kaushik, Zihao Xiao, Jiteng Mu, and Alan L. Yuille. Learning part
 750 segmentation from synthetic animals. In *WACV*, 2024.

751

752 Bryan A. Plummer, Liwei Wang, Chris M. Cervantes, Juan C. Caicedo, Julia Hockenmaier, and
 753 Svetlana Lazebnik. Flickr30k entities: Collecting region-to-phrase correspondences for richer
 754 image-to-sentence models. *IJCV*, 2017.

755

756 Dustin Podell, Zion English, Kyle Lacey, Andreas Blattmann, Tim Dockhorn, Jonas Müller, Joe
 757 Penna, and Robin Rombach. SDXL: improving latent diffusion models for high-resolution image
 758 synthesis. In *ICLR*. OpenReview.net, 2024.

759

760 Nikhila Ravi, Valentin Gabeur, Yuan-Ting Hu, Ronghang Hu, Chaitanya Ryali, Tengyu Ma, Haitham
 761 Khedr, Roman Rädle, Chloé Rolland, Laura Gustafson, Eric Mintun, Junting Pan, Kalyan Va-
 762 sudev Alwala, Nicolas Carion, Chao-Yuan Wu, Ross B. Girshick, Piotr Dollár, and Christoph
 763 Feichtenhofer. SAM 2: Segment anything in images and videos. *Arxiv*, 2024.

756 Realistic_Vision. realistic-vision-v51. <https://huggingface.co/stablediffusionapi/realistic-vision-v51>, 2023.

757
758
759 recraftAI. recraft. <https://www.recraft.ai/>, 2024.

760 Jonas Ricker, Dennis Assenmacher, Thorsten Holz, Asja Fischer, and Erwin Quiring. Ai-generated
761 faces in the real world: A large-scale case study of twitter profile images. In *RAID*, RAID '24,
762 2024.

763
764 riiwa. rRealism_v1.0_riiwa, 2024. URL <https://civitai.com/models/565139/rrealism?modelVersionId=629833>.

765
766 Robin Rombach, Andreas Blattmann, Dominik Lorenz, Patrick Esser, and Björn Ommer. High-
767 resolution image synthesis with latent diffusion models. In *CVPR*, 2022.

768
769 Andreas Rössler, Davide Cozzolino, Luisa Verdoliva, Christian Riess, Justus Thies, and Matthias
770 Nießner. Faceforensics++: Learning to detect manipulated facial images. In *ICCV*, 2019.

771
772 Haozhan Shen, Peng Liu, Jingcheng Li, Chunxin Fang, Yibo Ma, Jiajia Liao, Qiaoli Shen, Zilun
773 Zhang, Kangjia Zhao, Qianqian Zhang, Ruochen Xu, and Tiancheng Zhao. Vlm-r1: A stable and
774 generalizable r1-style large vision-language model, 2025.

775
776 Xincheng Shuai, Henghui Ding, Xingjun Ma, Rongcheng Tu, Yu-Gang Jiang, and Dacheng Tao. A
777 survey of multimodal-guided image editing with text-to-image diffusion models. *Arxiv*, 2024.

778
779 Oriane Siméoni, Huy V. Vo, Maximilian Seitzer, Federico Baldassarre, Maxime Oquab, Cijo Jose,
780 Vasil Khalidov, Marc Szafraniec, Seung Eun Yi, Michaël Ramamonjisoa, Francisco Massa, Daniel
781 Haziza, Luca Wehrstedt, Jianyuan Wang, Timothée Darcet, Théo Moutakanni, Lionel Sentana,
782 Claire Roberts, Andrea Vedaldi, Jamie Tolan, John Brandt, Camille Couprie, Julien Mairal, Hervé
783 Jégou, Patrick Labatut, and Piotr Bojanowski. Dinov3. *Arxiv*, 2025.

784
785 Chuangchuang Tan, Huan Liu, Yao Zhao, Shikui Wei, Guanghua Gu, Ping Liu, and Yunchao Wei.
786 Rethinking the up-sampling operations in cnn-based generative network for generalizable deepfake
787 detection. In *CVPR*, 2024a.

788
789 Chuangchuang Tan, Yao Zhao, Shikui Wei, Guanghua Gu, Ping Liu, and Yunchao Wei. Frequency-
790 aware deepfake detection: Improving generalizability through frequency space domain learning.
791 In *AAAI*, 2024b.

792
793 Bo Wang, Zhao Zhang, Suiyi Zhao, Xianming Ye, Haijun Zhang, and Meng Wang. Fakediffer:
794 Distributional disparity learning on differentiated reconstruction for face forgery detection. In
795 *AAAI*, 2025a.

796
797 Li Wang, Zheng Li, Xuhong Zhang, Shouling Ji, and Shanqing Guo. Faceswapguard: Safeguarding
798 facial privacy from deepfake threats through identity obfuscation. *Arxiv*, 2025b.

799
800 Chenfei Wu, Jiahao Li, Jingren Zhou, Junyang Lin, Kaiyuan Gao, Kun Yan, Shengming Yin, Shuai
801 Bai, Xiao Xu, Yilei Chen, Yuxiang Chen, Zecheng Tang, Zekai Zhang, Zhengyi Wang, An Yang,
802 Bowen Yu, Chen Cheng, Dayiheng Liu, Deqing Li, Hang Zhang, Hao Meng, Hu Wei, Jingyuan Ni,
803 Kai Chen, Kuan Cao, Liang Peng, Lin Qu, Minggang Wu, Peng Wang, Shuting Yu, Tingkun Wen,
804 Wensen Feng, Xiaoxiao Xu, Yi Wang, Yichang Zhang, Yongqiang Zhu, Yujia Wu, Yuxuan Cai,
805 and Zenan Liu. Qwen-image technical report. *Arxiv*, 2025.

806
807 Yuanjun Xiong, Kai Zhu, Dahua Lin, and Xiaoou Tang. Recognize complex events from static images
808 by fusing deep channels. In *CVPR*, 2015.

809
810 Shilin Xu, Xiangtai Li, Yanwei Li, Rui Yang, Tao Zhang, Yueyi Sun, Wei Chow, Linfeng Li, Hang
811 Song, Qi Xu, Yunhai Tong, and Hao Fe. Mixed-r1: Unified reward perspective for reasoning
812 capability in multimodal large language models. *Arxiv*, 2025.

813
814 Zhipei Xu, Xuanyu Zhang, Runyi Li, Zecheng Tang, Qing Huang, and Jian Zhang. Fakeshield:
815 Explainable image forgery detection and localization via multi-modal large language models.
816 *Arxiv*, 2024.

810 Zhiyuan Yan, Yong Zhang, Xinhang Yuan, Siwei Lyu, and Baoyuan Wu. Deepfakebench: A
 811 comprehensive benchmark of deepfake detection. In *NeurIPS*, 2023.

812

813 Zhiyuan Yan, Taiping Yao, Shen Chen, Yandan Zhao, Xinghe Fu, Junwei Zhu, Donghao Luo,
 814 Chengjie Wang, Shouhong Ding, Yunsheng Wu, and Li Yuan. DF40: toward next-generation
 815 deepfake detection. In *NeurIPS*, 2024.

816 Zhitao Yang, Zhongang Cai, Haiyi Mei, Shuai Liu, Zhaoxi Chen, Weiye Xiao, Yukun Wei, Zhongfei
 817 Qing, Chen Wei, Bo Dai, Wayne Wu, Chen Qian, Dahua Lin, Ziwei Liu, and Lei Yang. Synbody:
 818 Synthetic dataset with layered human models for 3d human perception and modeling. In *ICCV*,
 819 2023.

820 Jiahui Yu, Xin Li, Jing Yu Koh, Han Zhang, Ruoming Pang, James Qin, Alexander Ku, Yuanzhong
 821 Xu, Jason Baldridge, and Yonghui Wu. Vector-quantized image modeling with improved VQGAN.
 822 In *ICLR*, 2022.

823

824 Lingzhi Zhang, Zhengjie Xu, Connelly Barnes, Yuqian Zhou, Qing Liu, He Zhang, Sohrab Amirgh-
 825 odsi, Zhe Lin, Eli Shechtman, and Jianbo Shi. Perceptual artifacts localization for image synthesis
 826 tasks. In *ICCV*, 2023.

827 Tao Zhang, Xiangtai Li, Zilong Huang, Yanwei Li, Weixian Lei, Xueqing Deng, Shihao Chen,
 828 Shunping Ji, , and Jiashi Feng. Sa2va: Marrying sam2 with llava for dense grounded understanding
 829 of images and videos. *arXiv*, 2025.

830

831 Yue Zhang, Ben Colman, Xiao Guo, Ali Shahriyari, and Gaurav Bharaj. Common sense reasoning
 832 for deepfake detection. In *ECCV*, 2024.

833

834 Jinguo Zhu, Weiyun Wang, Zhe Chen, Zhaoyang Liu, Shenglong Ye, Lixin Gu, Hao Tian, Yuchen
 835 Duan, Weijie Su, Jie Shao, Zhangwei Gao, Erfei Cui, Xuehui Wang, Yue Cao, Yangzhou Liu,
 836 Xingguang Wei, Hongjie Zhang, Haomin Wang, Weiye Xu, Hao Li, Jiahao Wang, Nianchen Deng,
 837 Songze Li, Yinan He, Tan Jiang, Jiapeng Luo, Yi Wang, Conghui He, Botian Shi, Xingcheng
 838 Zhang, Wenqi Shao, Junjun He, Yingtong Xiong, Wenwen Qu, Peng Sun, Penglong Jiao, Han Lv,
 839 Lijun Wu, Kaipeng Zhang, Huipeng Deng, Jiaye Ge, Kai Chen, Limin Wang, Min Dou, Lewei Lu,
 840 Xizhou Zhu, Tong Lu, Dahua Lin, Yu Qiao, Jifeng Dai, and Wenhui Wang. Internvl3: Exploring
 advanced training and test-time recipes for open-source multimodal models, 2025.

841

842 Mingjian Zhu, Hanting Chen, Qiangyu Yan, Xudong Huang, Guanyu Lin, Wei Li, Zhijun Tu, Hailin
 843 Hu, Jie Hu, and Yunhe Wang. Genimage: A million-scale benchmark for detecting ai-generated
 844 image. In *NeurIPS*, 2023.

845

846

847

848

849

850

851

852

853

854

855

856

857

858

859

860

861

862

863

864 **A APPENDIX**
865866
867 **Contents of the Appendix:**

868 Section B provides full details on dataset construction, including:
869
870 - The generative methods used in this paper (Section B.1),
871 - The selection of caption models (Section B.2),
872 - Human expert assessment, including source image filtering, model choice, and generative quality
873 evaluation (Section B.3),
874 - Construction of the cold start dataset (Section B.4),
875 - The process of generating the ground-truth explanations (Section B.5).

876 Section C presents benchmark analyses, including:
877

878 - Dataset statistics and distributional comparisons (Section C.1),
879 - Cross-domain generalization analysis (Section C.2),
880 - Category-level and forgery-type asymmetry studies (Section C.3),
881 - Representative dataset samples (Section C.4),
882 - **Duplicate detection analysis (Section C.5).**

883 Section D outlines experimental settings and method details, including:
884

885 - Reinforcement learning configuration (Section D.1),
886 - Implementation settings (Section D.2),
887 - Qualitative comparison on tampered cases (Section D.3),
888 - Additional qualitative examples (Section D.4).

889 Section E discusses the broader social impact of our work.
890

891 **B DATA CONSTRUCTION**
892

893 In this section, we present the construction pipeline of the So-Fake dataset. We first describe
894 the generative methods employed to synthesize both fully synthetic and tampered images in So-
895 Fake-Set and So-Fake-OOD (Section B.1). We then detail the selection of caption models used to
896 provide textual descriptions images (Section B.2). Next, we outline the human expert assessment
897 procedure, including source filtering, model validation, and quality control (Section B.3). We
898 further introduce the cold start dataset designed to initialize reasoning capabilities with structured
899 annotations (Section B.4). Finally, we describe the generation of explanation ground-truths, which
900 serve as reliable supervision for evaluating model outputs (Section B.5).

901 **B.1 GENERATIVE METHODS**
902

903 We describe the generative models and prompting strategies used to synthesize both fully synthetic
904 and tampered images in So-Fake-Set and So-Fake-OOD, as shown in Table 9. In total, we employ 40
905 generative methods to ensure the dataset is comprehensive and diverse. To maintain architectural
906 balance, we include a range of both GAN-based and diffusion-based models. While some methods are
907 relatively outdated, a limited number are retained to reflect historical trends and enhance robustness.
908 For more advanced models such as FLUX (Labs, 2024), SD-3.5 (Esser et al., 2024), SD-XL (Podell
909 et al., 2024), and Latent Diffusion (Rombach et al., 2022), we generate a larger volume of samples
910 due to their accessibility and high visual fidelity.

918
919 Table 9: Details of generative methods used in constructing So-Fake-Set and So-Fake-OOD. Column
920 abbreviations: Set = So-Fake-Set, OOD = So-Fake-OOD, F = fully synthetic images, T = tampered
921 images. Real data source abbreviations: F30k = Flickr30k, OI = OpenImages, OF = OpenForensics.

ID-Number	Method	Model Type	Data Used	Generation Target	Year	Venue	Real Data Source	Data Scale	Code Link
1	Absolute-Reality (Lykton, 2023)	Diffusion	Set	F	2023	None	F30k & WIDER	50000	Hyper-link
2	AttGAN (He et al., 2017)	GAN	Set	F	2017	PAMI	FFHQ & CelebA	2000	Hyper-link
3	BEGAN (Berthelot et al., 2017)	GAN	Set	F	2017	NeurIPS	FFHQ & CelebA	2000	Hyper-link
4	Collaborative Diffusion (Huang et al., 2023)	Diffusion	Set	F	2023	CVPR	FFHQ & CelebA	30000	Hyper-link
5	CramerGAN (Bellelmar et al., 2017)	GAN	Set	F	2017	NeurIPS	FFHQ & CelebA	2000	Hyper-link
6	DiT-XL (Peebles & Xie, 2023)	Diffusion	Set	F	2023	ICCV	FFHQ & CelebA	10000	Hyper-link
7	FLUX1.1-dev (Labs, 2024)	Diffusion	Set	F & T	2024	None	FFHQ & CelebA & OI & COCO & OF	350000+	Hyper-link
8	InfoMaxGAN (Lee et al., 2021)	GAN	Set	F	2021	WACV	FFHQ & CelebA	2000	Hyper-link
9	Kandinsky3 (Arkhikpin et al., 2023)	Diffusion	Set	F	2023	None	F30k & WIDER	80000	Hyper-link
10	Latent diffusion (Rombach et al., 2022)	Diffusion	Set	F & T	2022	CVPR	F30k & WIDER & COCO & OI	250000+	Hyper-link
11	MMDGAN (Li et al., 2017)	GAN	Set	F	2017	NeurIPS	FFHQ & CelebA	2000	Hyper-link
12	playground (Li et al., 2024a)	Diffusion	Set	F	2024	None	F30k & WIDER	50000	Hyper-link
13	R3GAN (Huang et al., 2024a)	GAN	Set	F	2024	NeurIPS	FFHQ & CelebA	30000	Hyper-link
14	RDDM (Li et al., 2024)	Diffusion	Set	F	2024	CVPR	FFHQ & CelebA	10000	Hyper-link
15	rRealism_riiwa (riiwa, 2024)	Diffusion	Set	F	2024	None	F30k & WIDER	50000	Hyper-link
16	ReIGAN (Nie et al., 2019)	GAN	Set	F	2019	ICLR	FFHQ & CelebA	2000	Hyper-link
17	SD-3.5 (Esser et al., 2024)	Diffusion	Set	F	2024	ICML	FFHQ & CelebA & OI & COCO & F30k	100000+	Hyper-link
18	SD-XL (Podell et al., 2024)	Diffusion	Set	F & T	2024	ICLR	F30k & WIDER & COCO & OF	300000+	Hyper-link
19	StyleGAN-2 (Karras et al., 2020)	GAN	Set	F	2020	CVPR	FFHQ & CelebA	30000	Hyper-link
20	StyleGAN-3 (Karras et al., 2021a)	GAN	Set	F	2021	NeurIPS	FFHQ & CelebA	30000	Hyper-link
21	StyleGAN-XL (Podell et al., 2024)	GAN	Set	F	2022	SIGGRAPH	FFHQ & CelebA	30000	Hyper-link
22	SiT-XL (Mo et al., 2024)	Diffusion	Set	F	2024	ECCV	FFHQ & CelebA	10000	Hyper-link
23	SNGAN (Miyato et al., 2018)	GAN	Set	F	2018	ICLR	FFHQ & CelebA	2000	Hyper-link
24	STGAN (Liu et al., 2019)	GAN	Set	F	2019	CVPR	FFHQ & CelebA	2000	Hyper-link
25	VOGAN (Yu et al., 2022)	GAN	Set	F	2022	ICLR	FFHQ & CelebA	2000	Hyper-link
26	OpenForensics (Le et al., 2021)	GAN	Set	F	2021	CVPR	Google Open Images	10000	Hyper-link
27	Realistic Vision (Realistic.Vision, 2023)	Diffusion	Set	F	2023	None	F30k & WIDER & COCO & OF	50000	Hyper-link
28	FLUX1.1-Kontext-dev (Labs, 2024)	Diffusion	Set	F	2025	None	OI	8000+	Hyper-link
29	Qwen-image (Wu et al., 2025)	Diffusion	Set	F	2025	Arxiv	OI	3000+	Hyper-link
30	Midjourney (Midjourney, 2023)	Diffusion	Set	F	2023	None	OI	8000+	Hyper-link
31	Recraft-v3 (refractAI, 2024)	Diffusion	OOD	F	2024	None	Reddit	5000+	Hyper-link
32	GPT-4o(OpenAI, 2023)	Diffusion	OOD	F & T	2025	Arxiv	Reddit	8000+	Hyper-link
33	Image3 (Baldrige et al., 2024)	Diffusion	OOD	F	2025	Arxiv	Reddit	3000+	Hyper-link
34	Image4 (Baldrige et al., 2024)	Diffusion	OOD	F	2025	Arxiv	Reddit	3000+	Hyper-link
35	Nano Banana (Baldrige et al., 2024)	Diffusion	OOD	F	2025	None	Reddit	2000+	Hyper-link
36	Seedteam3.0 (Guo et al., 2025)	Diffusion	OOD	F	2025	Arxiv	Reddit	5000+	Hyper-link
37	Ideogram3.0 (Ideogram, 2025)	Diffusion	OOD	F & T	2025	None	Reddit	5000+	Hyper-link
38	Ideogram2.0 (Ideogram, 2024)	Diffusion	OOD	F	2024	None	Reddit	5000+	Hyper-link
39	FLUX1.1_pro (Labs, 2025)	Diffusion	OOD	F	2025	None	Reddit	3000+	Hyper-link
40	Hi-Dream (HiDream-ai, 2025)	Diffusion	OOD	F	2025	None	Reddit	3000+	Hyper-link

Table 10: Comparison of image captioning models for prompt generation using CLIP score.

Method	Mean±Std
Qwen2.5-VL-7B	0.3361±0.034
InternVL2-7B	0.3258±0.034
BLIP-2	0.3047±0.036
InstructBLIP	0.2996±0.034
LLaVA-7B	0.2974±0.037

B.2 CAPTION MODEL SELECTION

To ensure high-quality prompts for diffusion-based text-to-image synthesis, we first evaluate multiple captioning models on their ability to produce detailed descriptions of source images. Specifically, we randomly sample 1,000 images from So-Fake-Set and use five popular image captioning LLMs to generate corresponding prompts. We then compare prompt quality using CLIP similarity score, as shown in Table 10. The results show that Qwen2.5-VL-7B (Bai et al., 2025) achieves the highest CLIP score, and we therefore adopt it as our unified prompt generator for So-Fake.

B.3 HUMAN EXPERT ASSESSMENT

We conducted a rigorous human evaluation to ensure the quality and appropriateness of our dataset. Five experts participated in a multi-stage process that included: (1) filtering source images, (2) validating model selection choices, and (3) assessing the quality of generated synthetic content. The overall process is illustrated in Figure 6.

Source Image Filtering. To construct a realistic and diverse OOD benchmark, we carefully selected subreddits based on their popularity, topical diversity, and coverage of broad content categories representative of typical social media platforms. Specifically, we selected 11 subreddits, including (1) `pics`, (2) `HumanPorn`, (3) `aww`, (4) `EarthPorn`, (5) `Getsdraw`, (6) `Drawme`, (7) `TheWayWeWere`, (8) `Animal`, (9) `Ittookapicutre`, (10) `Sports`, and (11) `cityporn`. We

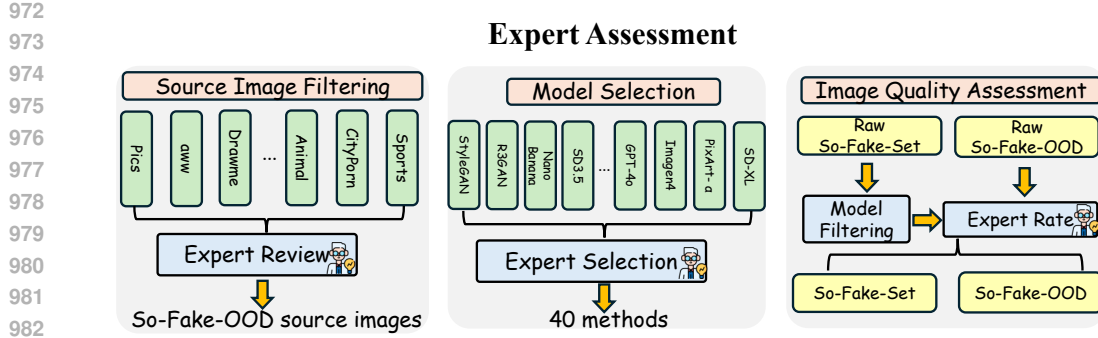


Figure 6: Human expert assessment process comprising **source image filtering**, **model selection**, and **image quality assessment**. This multi-stage evaluation ensures the dataset’s authenticity, diversity, and high visual quality for realistic deepfake detection scenarios.

used the official Reddit API³ to collect images and adhered to Reddit’s Public Content Policy⁴, ensuring that all images were used strictly for non-commercial research purposes.

After collecting the initial dataset, experts manually reviewed the Reddit images and filtered out those deemed inappropriate, harmful, or irrelevant to social media image analysis. This process resulted in a curated set of 100K high-quality source images for building the So-Fake-OOD benchmark.

Model Selection. Five human experts conducted a thorough evaluation of generative models to determine which should be included in So-Fake-Set and So-Fake-OOD. Each candidate model was reviewed based on its visual output quality, prompt controllability, content diversity, and relevance to current generative trends. The experts considered both widely adopted and emerging models, ensuring a balanced mix of GAN-based and diffusion-based architectures. This process resulted in the selection of 40 models, ranging from early GANs like StyleGAN and AttGAN to state-of-the-art diffusion models such as SD-XL (Podell et al., 2024), FLUX (Labs, 2024), and DiT (Peebles & Xie, 2023). By involving domain experts in model evaluation, we ensured that the final selection reflects both high technical quality and representative diversity for real-world image forgery scenarios.

Image Quality Assessment. Expert reviewers assessed the realism of generated images using a five-point scale (0–5, with 5 indicating the highest quality). Images scoring below 3 underwent secondary review, and confirmed low-quality samples were excluded from the dataset. For So-Fake-Set, we adopted a two-stage filtering process: an initial automated pass using QwenVL-7B (Bai et al., 2025) to remove clearly non-photorealistic images, followed by random human spot-checks. In contrast, all So-Fake-OOD images were subjected to a comprehensive manual review to ensure consistently high visual quality and realism. An illustrative example is provided in Figure 7.

B.4 COLD-START DATASET CONSTRUCTION

To initialize the reasoning capabilities of So-Fake-R1, we constructed a dedicated cold-start dataset. Our goal in this stage was not to maximize scale, but to establish a compact yet diverse corpus that provides consistent supervision signals and prevents overfitting.

Sampling strategy. We evenly sampled images from So-Fake-Set across all 30 generative methods and 12 semantic categories, ensuring broad coverage of both content and generation styles. In total, we curated approximately 9,000 images, deliberately balanced across the three classes (real, fully synthetic, tampered).

Annotation process. For each selected image, we obtained chain-of-thought explanations using GPT-4o (Hurst et al., 2024), chosen for its strong visual reasoning and descriptive capabilities. The prompts

³<https://www.reddit.com/prefs/apps>

⁴https://www.reddit.com/r/reddit/comments/1co0xnu/sharing_our_public_content_policy_and_a_new/

	Generator	Analysis	Score
1026			
1027			
1028		Blurry facial edges, missing details.	2,1,2,2,3
1029			
1030			
1031			
1032			
1033			
1034			
1035			
1036			
1037		Mostly natural, but noticeable inconsistencies (e.g., cow's shape)	3,3,4,3,3
1038			
1039			
1040			
1041			
1042		Rich details, overall photorealistic.	5,4,5,5,5
1043			
1044			
1045			
1046			
1047			
1048			

Figure 7: Illustrative examples of generation quality and reviewer scores at low, medium, and high quality levels.

followed a structured template (Listing 1), designed to elicit hierarchical rationales highlighting at least five concrete visual cues. For tampered images, we additionally attached bounding box coordinates derived from the corresponding binary manipulation masks, where the box was computed by extracting the extreme pixel coordinates (top-left and bottom-right) of the altered region. The standardized format "TAMPERED, <|box_start|>" $(x_1, y_1), (x_2, y_2)$ "<|box_end|>" allows models to explicitly associate textual justifications with localized manipulated regions.

Quality control. Although the explanations were generated automatically, we conducted lightweight human verification to ensure semantic consistency and adherence to the prescribed output format. Outputs exhibiting ambiguity or structural errors were removed. This procedure provided a high-confidence set of supervision signals without incurring the cost of large-scale manual annotation.

Listing 1: Prompt templates used for constructing the cold-start dataset.

```

PROMPT_TEMPLATES = {
    "REAL": """<image>

You are a forensic image analyst.

This image is known to be **real** (unaltered and directly from a
camera).

TASK:
In <= 1024 characters, describe at least five concrete visual
cues from this specific image that indicate it is authentic
and unedited.

The first sentence should depict the details of the given image.

OUTPUT FORMAT:
Return exactly two blocks:

```

```

1080 1) <think> ...your entire reasoning here... </think>
1081 2) <answer> REAL </answer>
1082
1083 EXAMPLE:
1084 <think>The image shows a woman with voluminous, side-swept wavy
1085 hair, wearing makeup and gazing slightly to the right.
1086 Several visual cues suggest the image is authentic and
1087 unedited: natural, consistent shadows across the face;
1088 realistic skin texture and tonal variation; hair strands
1089 blending smoothly into the background without abrupt edges;
1090 natural facial depth around the nose and cheekbones; and no
1091 signs of digital artifacts or unnatural
1092 blending.</think><answer>REAL</answer>
1093
1094 Now analyze the current image and respond using the exact format
1095 specified above.
1096 """
1097
1098 "TAMPERED": """<image>
1099 <mask>
1100
1101 You are a forensic image analyst.
1102 You will receive two images. The first image has been
1103     **tampered**. The second image is a binary mask (white =
1104     altered pixels) showing the tampered area of the first image.
1105
1106 TASK:
1107 In <= 1024 characters, first describe the scene, then describe at
1108     least five concrete manipulation clues visible around the
1109     highlighted area (e.g., lighting mismatch, edge artifacts).
1110 Do **not** mention the mask file itself.
1111
1112 OUTPUT FORMAT:
1113 Return exactly two blocks:
1114 1) <think> ...your entire reasoning here... </think>
1115 2) <answer> TAMPERED </answer>
1116
1117 EXAMPLE:
1118 <think>The image shows a crowded subway station where people are
1119     lined up near the platform doors, with a woman prominently
1120     posed in front holding a drink. Manipulation clues include a
1121     lighting mismatch on the woman compared to the ambient scene,
1122     hard edge artifacts around her silhouette, inconsistent
1123     shadowing beneath her, sharper resolution than surrounding
1124     elements, and slight scale distortion making her appear
1125     unnaturally inserted. The image is
1126     tampered.</think><answer>TAMPERED</answer>
1127
1128 Now analyze the current image and respond using the exact format
1129 specified above.
1130 """
1131
1132 "FULL_SYNTHETIC": """<image>
1133
1134 You are a forensic image analyst.
1135
1136 This image is known to be **fully synthetic** (entirely generated
1137     by AI).

```

```

1134
1135 TASK:
1136 In <= 1024 characters, describe at least five visual cues that
1137 reveal the image was generated artificially.
1138 The first sentence should depict the details of the given image.
1139
1140 OUTPUT FORMAT:
1141 Return exactly two blocks:
1142 1) <think> ...your entire reasoning here... </think>
1143 2) <answer> FULL_SYNTHETIC </answer>
1144
1145 EXAMPLE:
1146 <think>The image shows a shirtless, muscular man with tattoos
1147 walking down a palm-lined street near parked cars. Telltale
1148 signs of AI generation include overly smooth skin texture,
1149 inconsistent lighting between subject and background,
1150 unnatural tattoo symmetry, subtly distorted vehicle details,
1151 and unrealistically perfect muscle definition. The image is
1152 fully synthetic.</think><answer>FULL_SYNTHETIC</answer>
1153
1154 Now analyze the current image and respond using the exact format
1155 specified above.
1156 """
1157 }

```

1158

1159

B.5 EXPLANATION GROUND-TRUTH GENERATION

1160

1161

To supervise the explanation component of So-Fake-R1, we constructed textual ground-truth rationales using a two-step process. First, we employed **Claude Opus 4.1** (light logo, 2025), which was selected due to its strong performance in long-form reasoning and stylistic consistency, to generate chain-of-thought explanations. Each prompt included the original image, the associated tampered region mask (for tampered samples only), and the ground-truth class label (REAL, TAMPERED, or FULL_SYNTHETIC). The model then produced reasoning traces in the required output format.

1162

1163

To ensure semantic reliability, a sample of 3,000 generated explanations was systematically reviewed by human experts. The evaluation applied three criteria:

1164

1165

(1) **Accuracy** – the rationale must correctly describe visual evidence in the image;

1166

1167

(2) **Clarity** – the explanation must be concise and unambiguous;

1168

1169

(3) **Consistency** – reasoning style and conclusions must remain coherent across similar cases.

1170

1171

Outputs that were ambiguous or structurally flawed were refined or discarded. The finalized annotations therefore provide a high-confidence benchmark for evaluating multimodal reasoning. Importantly, these ground-truth explanations are used *only for evaluation* and are distinct from the cold start annotations employed during training (Appendix B.4).

1172

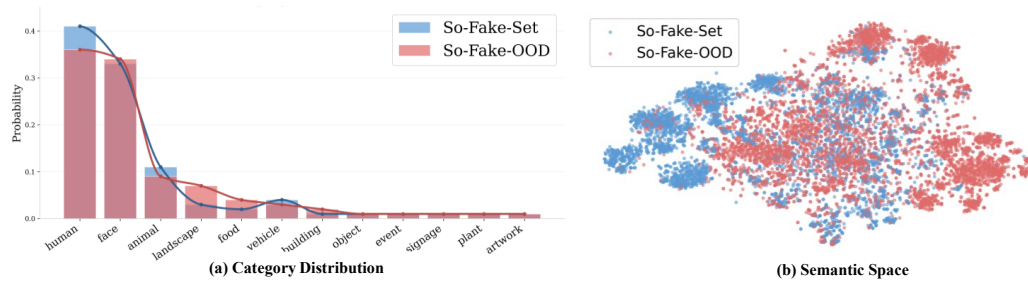
1173

C BENCHMARK ANALYSES

1174

1175

In this section, we conduct benchmark analyses to demonstrate the properties and utility of the So-Fake dataset. We begin with dataset statistics and distributional comparisons between So-Fake-Set and So-Fake-OOD (Section C.1). We then analyze cross-domain generalization to assess the challenges introduced by the OOD benchmark (Section C.2). Next, we examine category-level and forgery-type asymmetries to reveal systematic differences across semantic domains and manipulation modes (Section C.3). Finally, we provide representative examples that qualitatively illustrate the data types in So-Fake (Section C.4). Together, these analyses empirically substantiate the scale, diversity, and difficulty of So-Fake.

1188 C.1 DATASET STATISTICS AND DISTRIBUTIONAL COMPARISONS
11891200 Figure 8: Cross-domain alignment between So-Fake-Set and So-Fake-OOD. (a) Category distribution
1201 under the 12-class taxonomy. (b) CLIP embedding visualization.

1204 As outlined in Sec. 3.1, a valid OOD benchmark must maintain comparable semantic coverage while
1205 exhibiting measurable distributional shift, particularly in social media contexts. We analyze the
1206 relationship between So-Fake-Set and So-Fake-OOD to verify these properties, confirming both
1207 semantic alignment and realistic domain gap necessary for robust evaluation.

1208 **Category distribution:** under the unified 12-class taxonomy, the Jensen–Shannon divergence (JSD)
1209 is computed on the real subsets to avoid generation-induced artifacts. The divergence is low ($JSD \approx$
1210 0.08), indicating that So-Fake-OOD provides similar semantic coverage while avoiding category-
1211 driven bias in OOD evaluation, as illustrated in Figure 8 (a).

1212 **Semantic space:** CLIP embeddings are extracted from a randomly sampled subset of 10K images
1213 from each domain to capture overall semantic coverage. The embedding analysis shows substantial
1214 overlap between So-Fake-Set and So-Fake-OOD, while maintaining a measurable domain gap, as
1215 illustrated in Figure 8 (b).

1216 Together, these results demonstrate that So-Fake-Set and So-Fake-OOD are semantically aligned yet
1217 distributionally distinct, supporting fair and challenging OOD evaluation.

1219 Table 11: Cross-domain generalization performance on So-Fake-OOD using CNNSpot. ID = In-
1220 domain; OOD = Out-of-domain.

Category	Count	ID AUROC	OOD AUROC	Change (%)
GAN-based Methods	14	0.594	0.396	-19.8
Open-source Diffusion	7	0.584	0.471	-11.3
Commercial Diffusion	9	0.483	0.730	+24.7

1228 C.2 CROSS-DOMAIN GENERALIZATION ANALYSIS
1229

1230 To systematically analyze cross-domain generalization patterns, we categorize the 30 training methods
1231 into three groups based on their technical foundation and deployment context:

1232 **GAN-based models:** BEGAN, CramerGAN, InfoMaxGAN, MMDGAN, RelGAN, SNGAN,
1233 STGAN, AttGAN, VQGAN, StyleGAN2, R3GAN, StyleGAN3, StyleGAN-XL, OpenForensics_fake.

1234 **Open-source Diffusion Models:** Latent Diffusion, Collaborative Diffusion, DiT, RDDM, SiT, Stable
1235 Diffusion-3.5, Stable Diffusion-XL.

1236 **Commercial / Proprietary Diffusion Models:** FLUX.1-dev, FLUX-1-Kontext-dev, Kandinsky3,
1237 Midjourney, Playground, Qwen-image, Absolute_Reality, rRealism_riiwa, Realistic Vision.

1239 Our cross-domain evaluation reveals distinct generalization patterns that reflect the evolving technolog-
1240 ical landscape of social media forgery. As shown in Table 11 and Figure 5, while GAN-based
1241 methods achieve the strongest performance on So-Fake-Set, they exhibit substantial degradation
on So-Fake-OOD. Conversely, commercial diffusion models demonstrate the weakest performance

on the training domain but show remarkable cross-domain adaptation, achieving the highest OOD performance. Open-source diffusion models maintain moderate but stable performance.

These analyses capture an important transition in the landscape of social media forgeries. While GAN-based methods remain prevalent in targeted facial manipulations due to their controllability and efficiency, diffusion-based commercial models increasingly dominate the broader ecosystem by producing diverse, high-fidelity content across multiple categories. This technological stratification gives rise to asymmetric detection challenges: detectors trained primarily on academic GAN generators often underperform on emerging commercial diffusion models, whereas detectors exposed to commercial models exhibit more robust generalization across heterogeneous forgery sources.

The generalization gap between commercial and open source diffusion models reflects fundamental differences in their development contexts. Commercial generators face diverse real-world deployment pressures and continuous adversarial challenges in social media environments, leading to distributional properties that enhance detector generalizability. Open source diffusion models, while providing controlled experimental conditions and architectural diversity essential for research, may encode generator-specific artifacts that limit cross-domain transfer.

Importantly, although GAN-based models demonstrate limited OOD generalization, their inclusion remains essential for comprehensive evaluation. These models continue to drive many facial manipulation techniques prevalent on social media platforms, provide crucial contrast to diffusion-based methods that illuminates paradigm shifts in generative technology, and represent persistent threats that detection systems must handle in practice. Taken together, these findings underscore that future detection strategies should move beyond isolated, single-paradigm benchmarks. Effective systems require balanced coverage across both GAN-based and diffusion-based forgeries, supported by adaptive training protocols that account for the diverse threat landscape encountered in real-world deployment scenarios. By capturing the performance divergence between different generative paradigms, So-Fake provides a benchmark that reflects the complex and evolving nature of social media forgeries.

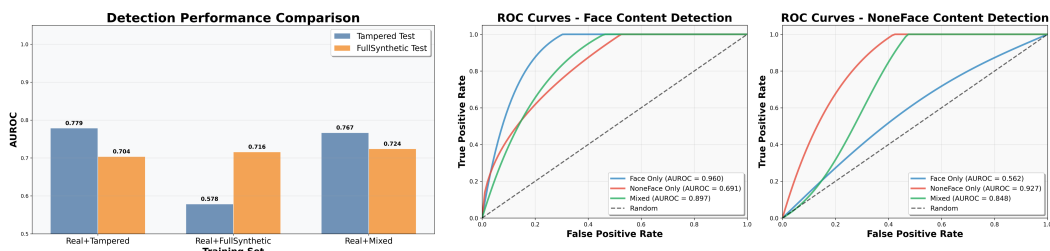


Figure 9: AUROC on tampered vs. full synthetic tests under different settings. Figure 10: ROC curves for face (left) and none face (right) tests.

C.3 CATEGORY-LEVEL AND FORGERY-TYPE ASYMMETRY STUDIES

In this section, we move beyond quantitative benchmarks to discuss two key aspects surfaced by So-Fake: (1) differences between tampered and fully synthetic forgeries and (2) the contrast between face-centric and non-face content. We report results using **CNNSpot** as the detector, given its broad adoption as a generator-agnostic baseline.

Tampered vs. Full Synthetic. Figure 9 reveals a significant transfer detection gap between tampered and fully synthetic forgeries. Detectors trained on tampered content perform well in-domain (0.779) but performed relatively poorly on synthetic data (0.704), while synthetic-trained models show the reverse pattern (0.578 vs. 0.716). This asymmetry suggests fundamentally different forensic signatures rather than a shared distribution. Mixed training bridges this gap (0.767 vs. 0.724), demonstrating that a unified three-class approach effectively captures both manipulation types while preserving generalization performance. This finding directly validates our design choice for social media forgery detection, where the coexistence of both manipulation types in user feeds necessitates robust cross-category generalization. Our three-class taxonomy (real, tampered, fully synthetic) mirrors the spectrum of fake content prevalent on social platforms, where subtle regional manipulations (e.g., localized inpainting) and entirely AI-generated posts coexist and require unified detection frameworks to ensure comprehensive coverage of real-world scenarios.

1296 **Face vs. Non-Face Forgeries.** Deepfake detection has traditionally centered on facial manipulations,
 1297 which constitute the majority of existing benchmarks and detection frameworks. To assess whether
 1298 this focus has created domain-specific biases, we examine detection performance across face and
 1299 non-face categories on our dataset. Our analysis reveals a clear asymmetry: face-centric forgeries are
 1300 substantially easier to detect than non-face ones, as shown in Figure 10. Specifically, models achieve
 1301 an AUROC of 0.960 on face content but only 0.562 on non-face content when trained exclusively
 1302 on faces, demonstrating a dramatic 39.8% performance drop. However, our integrated approach
 1303 combining faces with 11 diverse non-face categories yields improved overall robustness—mixed
 1304 training achieves balanced performance with face detection (AUROC = 0.897) and non-face detection
 1305 (AUROC = 0.848), representing a 28.6% improvement over face-only training on non-face content.
 1306 This design choice directly reflects social media reality, where users encounter heterogeneous content
 1307 spanning portraits, landscapes, objects, and events within the same feeds. By explicitly covering this
 1308 full spectrum, So-Fake provides a more realistic testbed that addresses the overlooked dimension of
 1309 generalizable forgery detection across diverse content types.
 1310



1311 Figure 11: Representative *real* images from So-Fake-Set (left) and So-Fake-OOD (right).
 1312
 1313
 1314
 1315
 1316
 1317
 1318
 1319
 1320
 1321
 1322
 1323
 1324
 1325
 1326
 1327
 1328

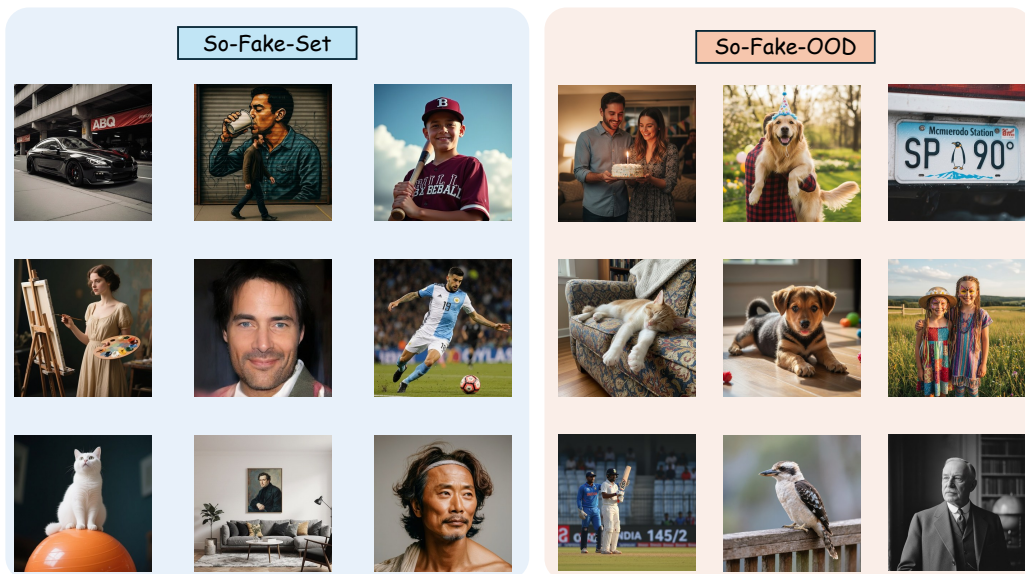
1334 C.4 REPRESENTATIVE DATASET SAMPLES

1335 In this section, we present representative samples from **So-Fake-Set** and **So-Fake-OOD**, covering the
 1336 three categories of our benchmark: *real* images from authentic sources, *tampered* images generated
 1337 by localized inpainting with masks, and *fully synthetic* images created by GANs and diffusion-based
 1338 models. Examples are shown in Figure 11 (real images), Figure 12 (tampered images), and Figure 13
 1339 (fully synthetic images).
 1340

1341 C.5 DUPLICATE DETECTION ANALYSIS

1343 To verify the independence between So-Fake-Set and So-Fake-OOD, we conducted comprehensive
 1344 similarity analysis using DINOv3 (ViT-L/16) Siméoni et al. (2025), a state-of-the-art self-supervised
 1345 vision model widely adopted for duplicate detection tasks. We evaluate duplicate similarity under the
 1346 following configuration:
 1347

1348 **Data sampling.** Due to computational constraints, we randomly sample 10% of the real images from
 1349 each split (seed = 42), resulting in 65,000 sampled real images from So-Fake-Set (650K total) and
 3,300 from So-Fake-OOD (33K total).

Figure 12: Representative *tampered* images from So-Fake-Set (left) and So-Fake-OOD (right).Figure 13: Representative *full synthetic* images from So-Fake-Set (left) and So-Fake-OOD (right).

Similarity metric: We compute cosine similarity from DINOv3 embeddings and apply a conservative threshold of 0.9 to identify potential duplicates.

Results. The experiment identified 19 high-similarity pairs across the two subsets. We manually inspected all 19 pairs, with representative examples shown in Figure 14. Visual inspection confirms these pairs represent distinct images exhibiting semantic or compositional similarity rather than actual duplication. For instance, Pair 1 shows two photographs of Moraine Lake captured under different lighting and weather conditions, Pair 2 depicts the same vehicle model photographed in different settings, and Pair 5 presents the same species rendered in different color spaces and environmental contexts.

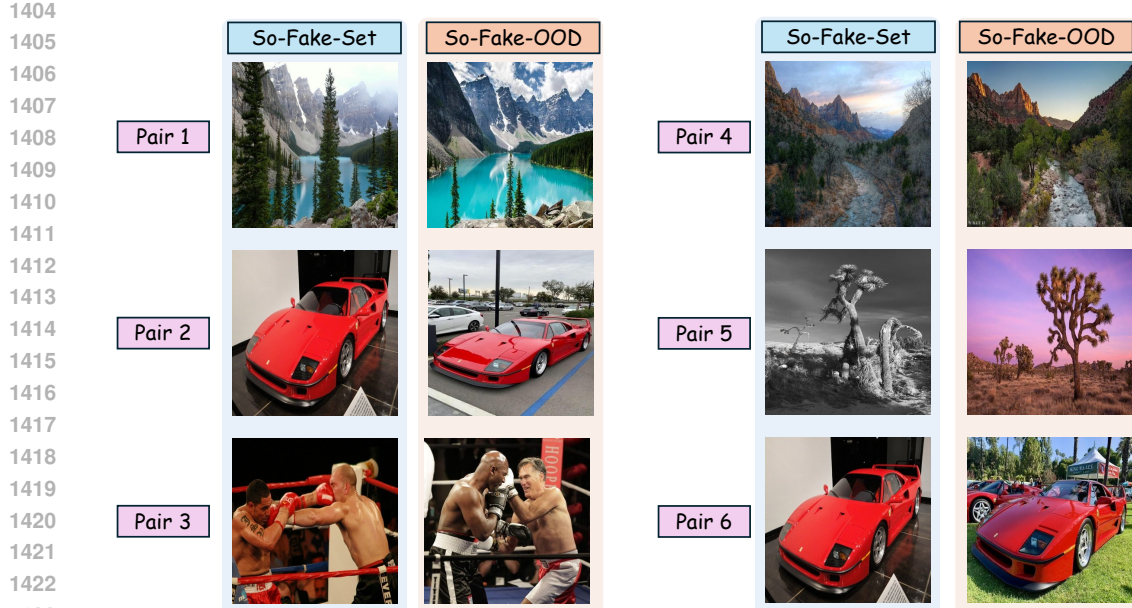


Figure 14: Representative high-similarity pairs identified by DINOv3 (cosine similarity ≥ 0.9) between So-Fake-Set and So-Fake-OOD. Visual inspection confirms these are distinct images with topic-level similarity rather than actual duplicates, demonstrating minimal overlap between the two splits.

These findings align with expected behavior when comparing large-scale image collections spanning overlapping semantic categories. The minimal overlap rate (19 pairs from 68,300 cross-dataset comparisons, representing 0.028%) confirms that So-Fake-Set and So-Fake-OOD maintain strong distributional independence, validating So-Fake-OOD as a rigorous out-of-distribution benchmark.

D EXPERIMENTAL SETTINGS AND METHOD DETAILS

In this section, we provide comprehensive implementation details for the So-Fake-R1 framework and experimental configurations used throughout our evaluation. We begin by detailing the reinforcement learning setup, including reward function specifications, training hyperparameters, and optimization procedures (Section D.1). We then outline the implementation specifics for both the baseline methods and our proposed approach, covering model architectures, training protocols, and computational requirements (Section D.2). To further contextualize our contributions, we include a comparative visualization of tampered cases across So-Fake-R1 and competing detectors, highlighting differences in localization quality (Section D.3). Finally, we present additional qualitative examples that illustrate the detection, localization, and explanation capabilities of So-Fake-R1 across diverse forgery types and content categories (Section D.4). These details ensure reproducibility and provide practical guidance for researchers building upon our work.

D.1 REINFORCEMENT LEARNING CONFIGURATION

As shown in Figure 15, the GRPO training is the core of So-Fake-R1. In this section, we describe the configuration of the GRPO training setup, including the specific weight assignments and detailed reward components. We first discuss the rationale for applying GRPO to multi-modal tasks, then provide detailed specifications of our reward function design and individual reward components.

GRPO for Multi-modal Tasks. Reinforcement learning has recently shown promise in vision-language tasks by enabling models to develop reasoning capabilities through trial-and-error learning rather than mimicking human-provided explanations. Among recent advances, Group Relative Policy

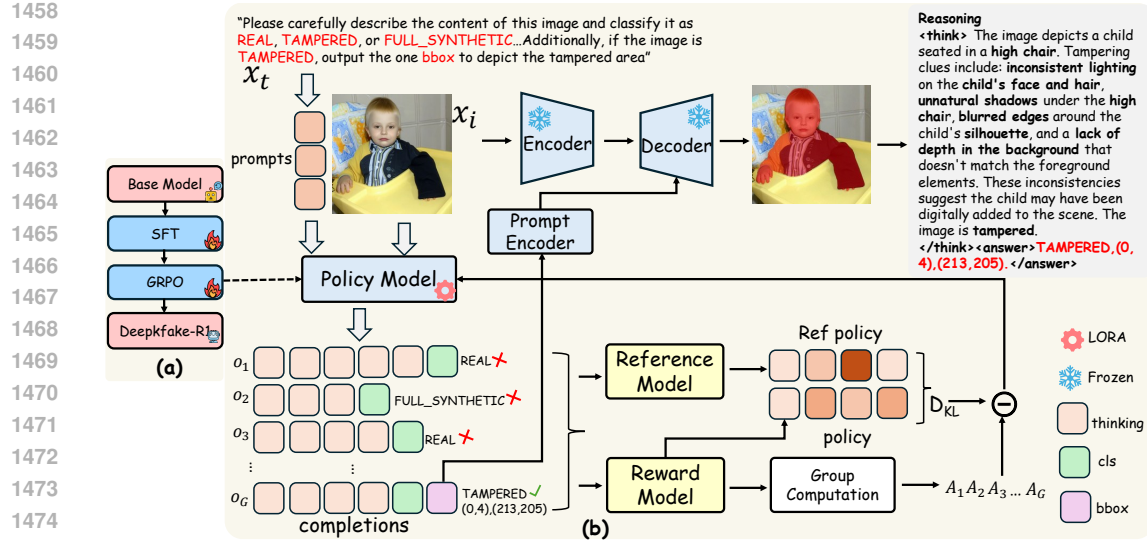


Figure 15: (a): Overview of the So-Fake-R1 training process; (b): The detailed So-Fake-R1 GRPO training process. The example shows a tampered image where a boy has been manipulated.

Table 12: Ablation study on reward weight configurations.

λ_{fmt}	λ_{cls}	$\lambda_{\text{seg_fmt}}$	λ_{IoU}	λ_{L1}	Detection(Acc)	Localization(IoU)
1.0	1.0	1.0	1.0	1.0	91.8	45.2
0.1	0.9	0.1	0.9	0.9	93.2	48.6
0.5	1.0	0.5	1.0	1.0	92.1	46.8

Optimization (GRPO) (DeepSeek-AI et al., 2025) has emerged as particularly effective for tasks requiring minimal human supervision, achieving this through rule-based reward mechanisms that guide models toward desired behaviors without relying on extensive annotations. This annotation-free approach makes GRPO particularly valuable for vision-language models (VLMs) (Zhang et al., 2025; Huang et al., 2025a; Xu et al., 2025), where obtaining detailed human explanations for visual reasoning is especially challenging. Notable applications include Seg-Zero (Liu et al., 2025a) for zero-shot segmentation, Visual-RFT (Liu et al., 2025b) for visual question answering, and VLM-R1 (Shen et al., 2025) for robust object detection, establishing GRPO as a standard approach for optimizing multi-modal models that require balancing multiple objectives.

Our reward function design follows established practices in multi-modal reinforcement learning: (1) format rewards ensure structured outputs, which is standard for all structured generation tasks; (2) task-specific rewards based on ground truth labels, following the standard practice of supervised-to-RL conversion; and (3) multi-metric combinations (IoU + L1) that align with established practices in object detection literature. Although GRPO has shown success in various vision-language tasks, it has not yet been applied to forgery detection, where both accuracy and unbiased explainability are essential. To our knowledge, So-Fake-R1 is the first framework to use GRPO for forgery detection.

Reward Function Design. The total reward is computed as:

$$R_{\text{total}} = \lambda_{\text{fmt}} R_{\text{fmt}} + \lambda_{\text{cls}} R_{\text{cls}} + \lambda_{\text{seg_fmt}} R_{\text{seg_fmt}} + \lambda_{\text{IoU}} R_{\text{IoU}} + \lambda_{\text{L1}} R_{\text{L1}} \quad (2)$$

Based on observations from the ablation study on reward design (Table 7), we found that the progress of GRPO training is less sensitive to formatting rewards, which primarily serve as structural constraints rather than performance drivers. Therefore, we set $\lambda_{\text{fmt}} = \lambda_{\text{seg_fmt}} = 0.1$, and $\lambda_{\text{cls}} = \lambda_{\text{IoU}} = \lambda_{\text{L1}} = 0.9$, encouraging the model to prioritize classification accuracy and precise segmentation outputs during training. This weight allocation is empirically validated through Table 12, demonstrating that each component contributes to the final performance. Below, we detail each reward component:

1512 *Explanation Format Reward (R_{fmt})*. This reward function encourages structured reasoning by requiring
 1513 the model to format its output using `<think>...</think>` for the reasoning process and
 1514 `<answer>...</answer>` for the final answer. The model receives a reward of +1 if the output
 1515 follows this format correctly; otherwise, it receives 0. This follows the standard practice in structured
 1516 text generation tasks where format compliance is enforced through binary rewards.

1517 *Detection Reward (R_{cls})*. This reward encourages accurate multi-class classification among
 1518 REAL, TAMPERED, and FULL_SYNTHETIC, based on the label provided within the
 1519 `<answer>...</answer>` tags. The model receives a reward of +1 for correctly identifying REAL
 1520 or FULL_SYNTHETIC images, and a higher reward of +3 for correctly identifying TAMPERED, as
 1521 detecting tampered images is more challenging based on our preliminary analysis showing lower
 1522 baseline performance on this class. Incorrect classifications receive a reward of 0.

1523 *Localization Format Reward ($R_{seg,fmt}$)*. This reward ensures that bounding boxes follow a strict
 1524 coordinate specification. The model receives a reward of +1 if its output includes properly for-
 1525 matted coordinates (i.e., four numerical values enclosed between the tags `<|box_start|>` and
 1526 `<|box_end|>`), such as: `<|box_start|> (x1, y1), (x2, y2) <|box_end|>`. If the format is
 1527 incorrect or missing, the reward is 0.

1528 *IoU Reward (R_{IoU})*. This reward grants a positive score when predicted boxes achieve meaningful
 1529 overlap with ground truth. For TAMPERED images, the model receives a reward of +1 if the predicted
 1530 bounding box achieves an Intersection-over-Union (IoU) greater than 0.5 compared to the ground
 1531 truth. The 0.5 IoU threshold follows the standard practice in object detection literature for meaningful
 1532 overlap assessment. For REAL and FULL_SYNTHETIC images, which do not require localization, a
 1533 reward of +1 is assigned by default. In all other cases, the reward is 0.

1534 *L1 Reward (R_{L1})*. This reward further refines localization accuracy by rewarding predictions within
 1535 close proximity to ground truth coordinates. For TAMPERED images, the model receives a reward
 1536 of +1 if the total L1 distance across all four coordinates is less than 10 pixels. For REAL and
 1537 FULL_SYNTHETIC samples, which do not require bounding boxes, a default reward of +1 is
 1538 assigned. Otherwise, the reward is 0. The combination of IoU and L1 rewards ensures both region
 1539 overlap quality and precise boundary alignment, as IoU alone can be satisfied by oversized boxes.

D.2 IMPLEMENTATION DETAILS

1543 **Baseline Methods.** For detection-only methods including CnnSpot (Frank & Holz, 2021), Uni-
 1544 vFD (Ojha et al., 2023), FreAware (Tan et al., 2024b), and NPR (Tan et al., 2024a), we follow
 1545 the official implementation guidelines provided in their respective documentation and adopt the
 1546 recommended or highest-performing configurations when available.

1547 For image forgery detection and localization (IFDL) methods, we fine-tune TruFor (Guillaro et al.,
 1548 2023), PSCC-Net (Liu et al., 2022), and SIDA (Huang et al., 2025b) on So-Fake-Set according to the
 1549 official recommended settings. For FakeShield (Xu et al., 2024) and HIFI-Net (Guo et al., 2024), we
 1550 use the pre-trained weights for evaluation due to code availability constraints.

1551 For vision-language models, including LLaVA-1.5-
 1552 13B (Liu et al., 2023), InternVL3-8B (Zhu et al., 2025),
 1553 Qwen2.5-VL-7B (Bai et al., 2025), and DeepSeek-VL-
 1554 7B (DeepSeek-AI et al., 2025), we adopt the `ms-swift`⁵
 1555 framework for streamlined integration, fast inference, and
 1556 effective hyperparameter tuning. For each model, we se-
 1557 lect the best-performing checkpoint based on validation
 1558 performance. For LISA (Lai et al., 2024), we use the
 1559 official codebase and follow the authors' recommended
 1560 hyperparameter settings.

1561 **So-Fake-R1 Implementation.** We use Qwen2.5-VL-
 1562 7B-Instruct Bai et al. (2025) as our policy model and
 1563 SAM2 Ravi et al. (2024) for segmentation refinement. Our training follows a two-stage pipeline
 1564 comprising a cold-start phase followed by GRPO fine-tuning. In both stages, all input images (and

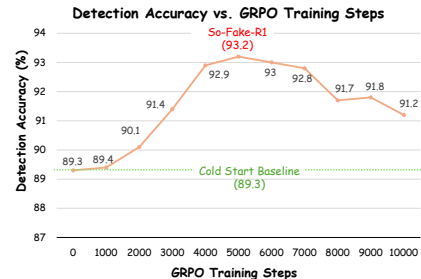


Figure 16: Detection accuracy over GRPO training steps.

⁵<https://github.com/modelscope/ms-swift>

1566 masks, when present) are resized to 224×224 pixels to ensure consistent input dimensions and
 1567 reduce memory consumption.

1568 For the cold-start phase, we apply LoRA (Hu et al., 2021) with $\alpha = 32$ and rank 16. The model is
 1569 trained using a learning rate of 5e-5, weight decay of 0.1, and a maximum token length of 2048. This
 1570 stage takes approximately 30 minutes to complete on a single A100 GPU (40GB).

1571 For the GRPO phase, we also apply LoRA with $\alpha = 32$ and rank 8. The model is trained with a
 1572 learning rate of 1e-4, a warmup ratio of 0.05, weight decay of 0.1, and a maximum token length
 1573 of 2048. We assign reward weights as $\lambda_{\text{fmt}} = \lambda_{\text{seg,fmt}} = 0.1$, and $\lambda_{\text{cls}} = \lambda_{\text{IOU}} = \lambda_{\text{L1}} = 0.9$ based
 1574 on Table 12. GRPO training is conducted on two A100 GPUs (40GB each) and completes in
 1575 approximately 24 hours. We select the checkpoint at 5000 training steps, as it achieves the best
 1576 overall performance across evaluation metrics, as shown in Figure 16.

1578 D.3 QUALITATIVE COMPARISON ON TAMPERED CASES

1580 We further provide a qualitative comparison of tampered cases against representative IFDL baselines.
 1581 As shown in Figure 17, So-Fake-R1 achieves more precise localization of manipulated regions, closely
 1582 matching the ground-truth masks. In contrast, competing methods often misidentify boundaries
 1583 or overlook subtle edited areas. These results highlight the effectiveness of our reinforcement
 1584 learning-based framework in capturing fine-grained tampering artifacts.

1585 D.4 ADDITIONAL QUALITATIVE EXAMPLES

1586 In this section, we present additional examples of So-Fake-R1’s outputs on the So-Fake-OOD
 1587 benchmark. Since So-Fake-R1 was not trained on this benchmark, the results include both successful
 1588 predictions and failure cases. To ensure fair representation, test images were randomly selected.
 1589 These examples illustrate the model’s generalization capabilities, highlight areas for improvement,
 1590 and suggest directions for future research. The qualitative examples are shown in Figures 18–25.

1593 E BROADER SOCIAL IMPACT

1595 To ensure quality, fairness, and responsible use, we incorporated multiple safeguards throughout the
 1596 development process. Expert reviewers were engaged at every stage, including the selection of source
 1597 content, the validation of generative outputs, and the refinement of textual explanations, to guarantee
 1598 both reliability and appropriateness. For So-Fake-OOD, we followed Reddit’s Public Content Policy
 1599 and applied multi-stage human filtering to exclude unsuitable or sensitive material. All datasets and
 1600 models are released strictly for non-commercial, research-only purposes under controlled access.

1602 So-Fake-Set, So-Fake-OOD, and So-Fake-R1 framework are designed to advance the field of multi-
 1603 modal forgery detection, with a particular focus on social media contexts. By offering large-scale,
 1604 diverse, and well-annotated benchmarks alongside an interpretable and high-performing model, our
 1605 work provides valuable resources for the research community. These contributions can support
 1606 future developments in robust AI systems, foster academic exploration, and assist in building more
 1607 trustworthy digital media ecosystems. We believe our dataset and methods will positively impact the
 1608 broader AI and computer vision communities by encouraging progress in transparent, explainable,
 1609 and socially beneficial technologies for image authenticity verification.

1610
 1611
 1612
 1613
 1614
 1615
 1616
 1617
 1618
 1619

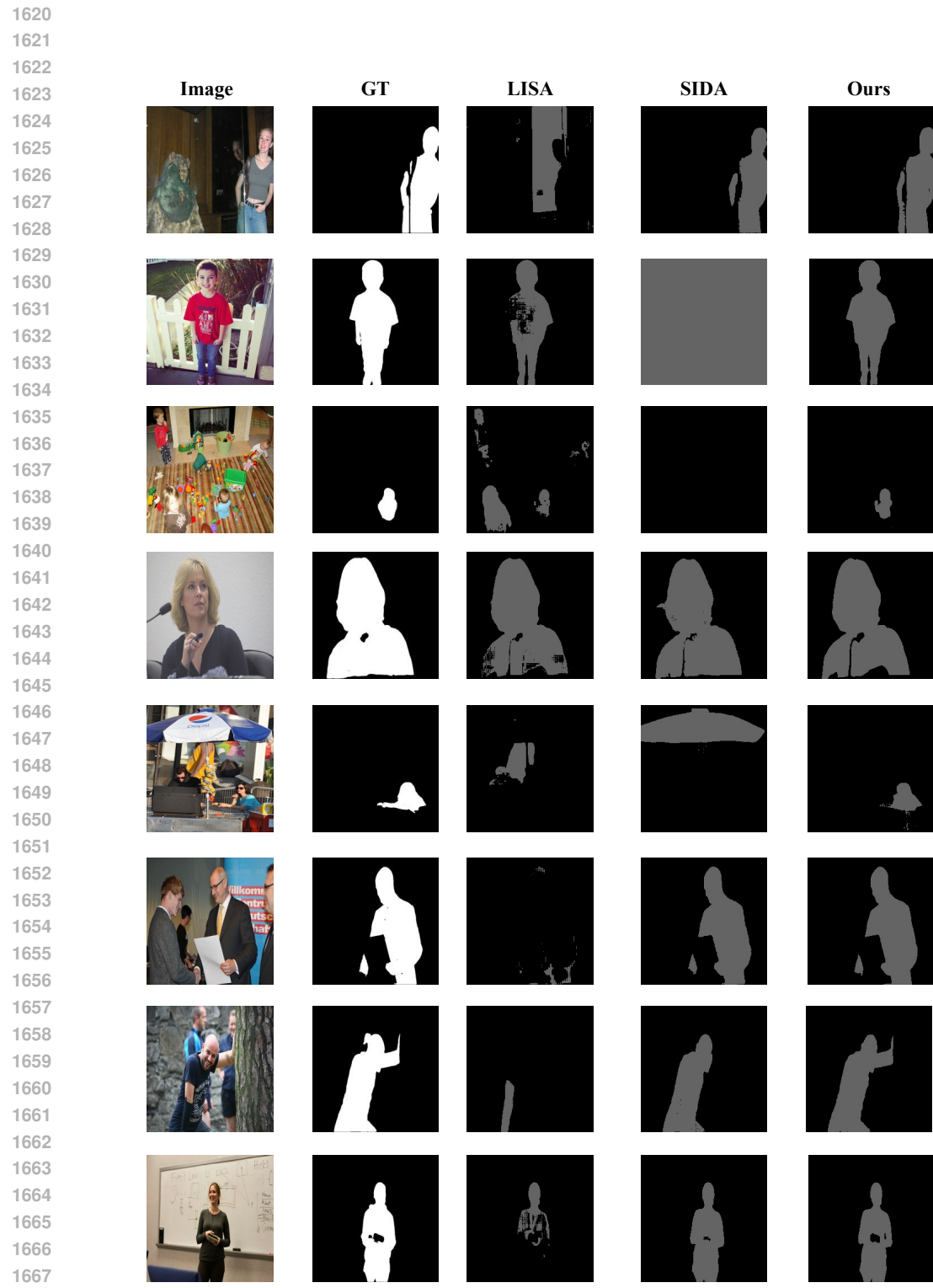


Figure 17: Qualitative comparison of tampered cases on **So-Fake-Set**, comparing ground-truth (GT), LISA, SIDA, and our So-Fake-R1.

1674

1675

1676

1677

1678

1679

1680

1681

1682

1683



"Please carefully describe the content of this image and classify it as **REAL**, **TAMPERED**, or **FULL_SYNTHETIC**... Additionally, if the image is **TAMPERED** output the one **bbox** to depict the tampered area"

1684

1685

1686

1687

1688

1689

1690

1691

1692

1693

1694

1695

1696

1697

1698

1699

1700

1701

1702

1703

1704

1705

1706

1707

1708

1709

1710

1711

1712

1713

1714

1715

1716

1717

1718

1719

1720

1721

1722

1723

1724

1725

1726

1727



correct



<think> The image shows an **older man holding a device close to his face**. Several visual cues suggest the image is authentic and unedited: the **lighting is natural**, casting **soft shadows** on his face; his **skin texture appears realistic** with subtle variations in tone; the device he holds has a **consistent shape** and color gradient typical of real objects; the background is blurred but **maintains a natural depth of field**; and there are **no visible digital artifacts** or unnatural blending that would indicate manipulation. </think><answer>REAL</answer>



failure

<think> The image depicts **four cats sitting on a wooden surface against a plain background**. Visual cues indicating authenticity include the **natural lighting that casts soft shadows and highlights** on the cats' fur, the **realistic texture and color variations** in their coats, the **subtle blending** of their fur tones, and the **absence of any digital artifacts** or unnatural blending. The cats' postures and expressions appear genuine, suggesting they were captured in a real-life setting rather than digitally created. </think><answer>REAL</answer>

Analysis: A fully synthetic image is misclassified as real, suggesting the model fails to detect subtle generative artifacts.



correct

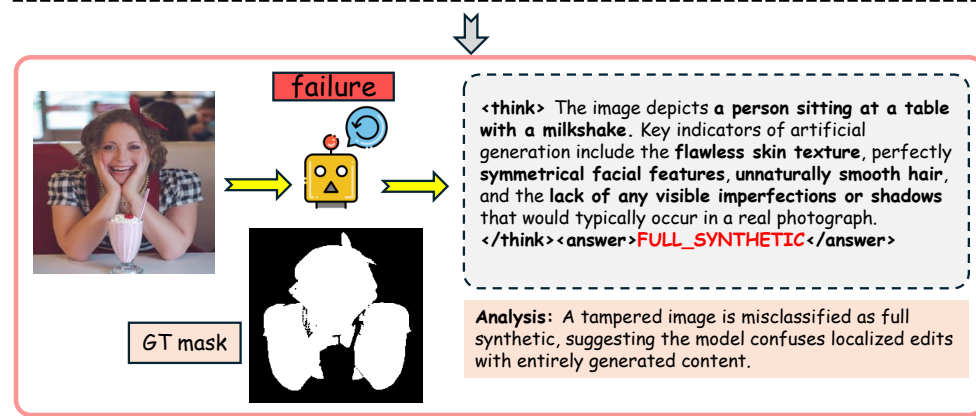
<think> The image depicts a **child in a white dress** with a **smooth, uniform texture** throughout the clothing and skin. The lighting appears **overly even** and **lacks natural shadows or highlights**. The hair has a **consistent, almost unnaturally smooth texture** without visible strands or highlights. The background is a **solid color** with **no discernible depth or texture**, suggesting a lack of real-world environmental elements. Lastly, the **overall composition and proportions seem slightly off**, hinting at artificial generation. </think><answer>FULL_SYNTHETIC</answer>

Figure 18: Qualitative results of So-Fake-R1 on the So-Fake-OOD benchmark.

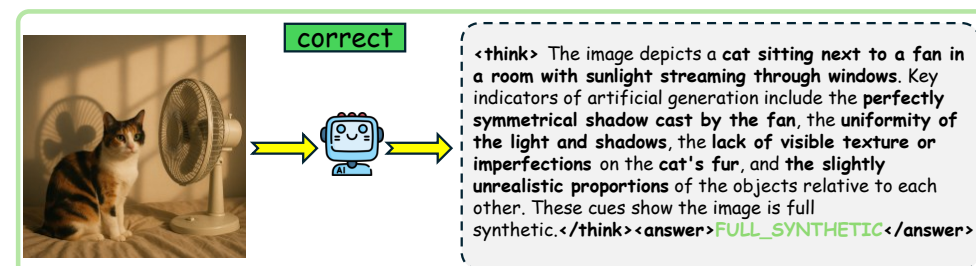
1728
1729
1730
1731
1732
1733
1734
1735
1736
1737

1738  "Please carefully describe the content of this image and classify it as **REAL**, **TAMPERED**, or **FULL_SYNTHETIC**... Additionally, if the image is **TAMPERED** output the one **bbox** to depict the tampered area"

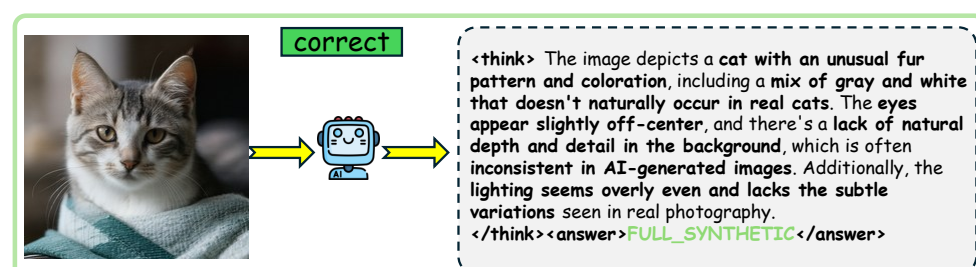
1739
1740
1741
1742
1743
1744
1745
1746
1747
1748
1749
1750
1751
1752



1753
1754
1755
1756
1757
1758
1759
1760
1761



1762
1763
1764
1765
1766
1767
1768
1769
1770



1771
1772
1773
1774
1775
1776
1777
1778
1779
1780
1781

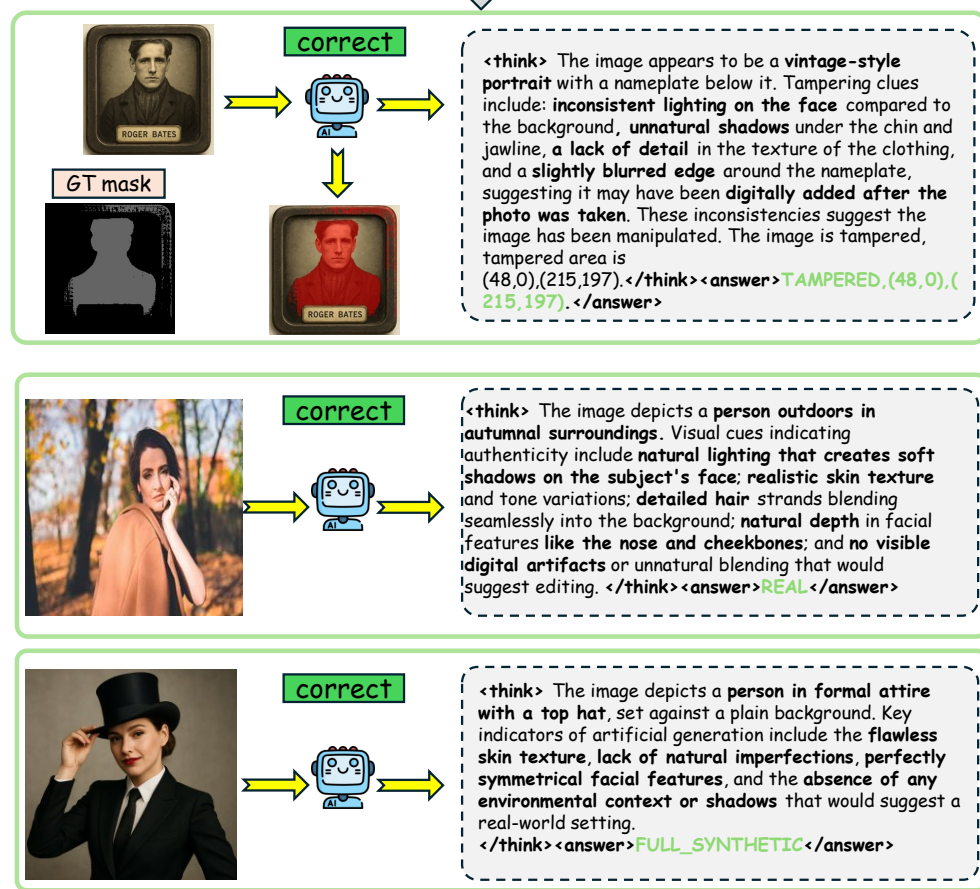
Figure 19: Qualitative results of So-Fake-R1 on the So-Fake-OOD benchmark.

1782
1783
1784
1785
1786
1787
1788
1789
1790
1791
1792



"Please carefully describe the content of this image and classify it as **REAL**, **TAMPERED**, or **FULL_SYNTHETIC**... Additionally, if the image is **TAMPERED** output the one **bbox** to depict the tampered area"

1793
1794
1795
1796
1797
1798
1799
1800
1801
1802
1803
1804
1805
1806
1807



1825
1826
1827
1828
1829
1830
1831
1832
1833
1834
1835

1836
1837
1838
1839
1840
1841
1842
1843

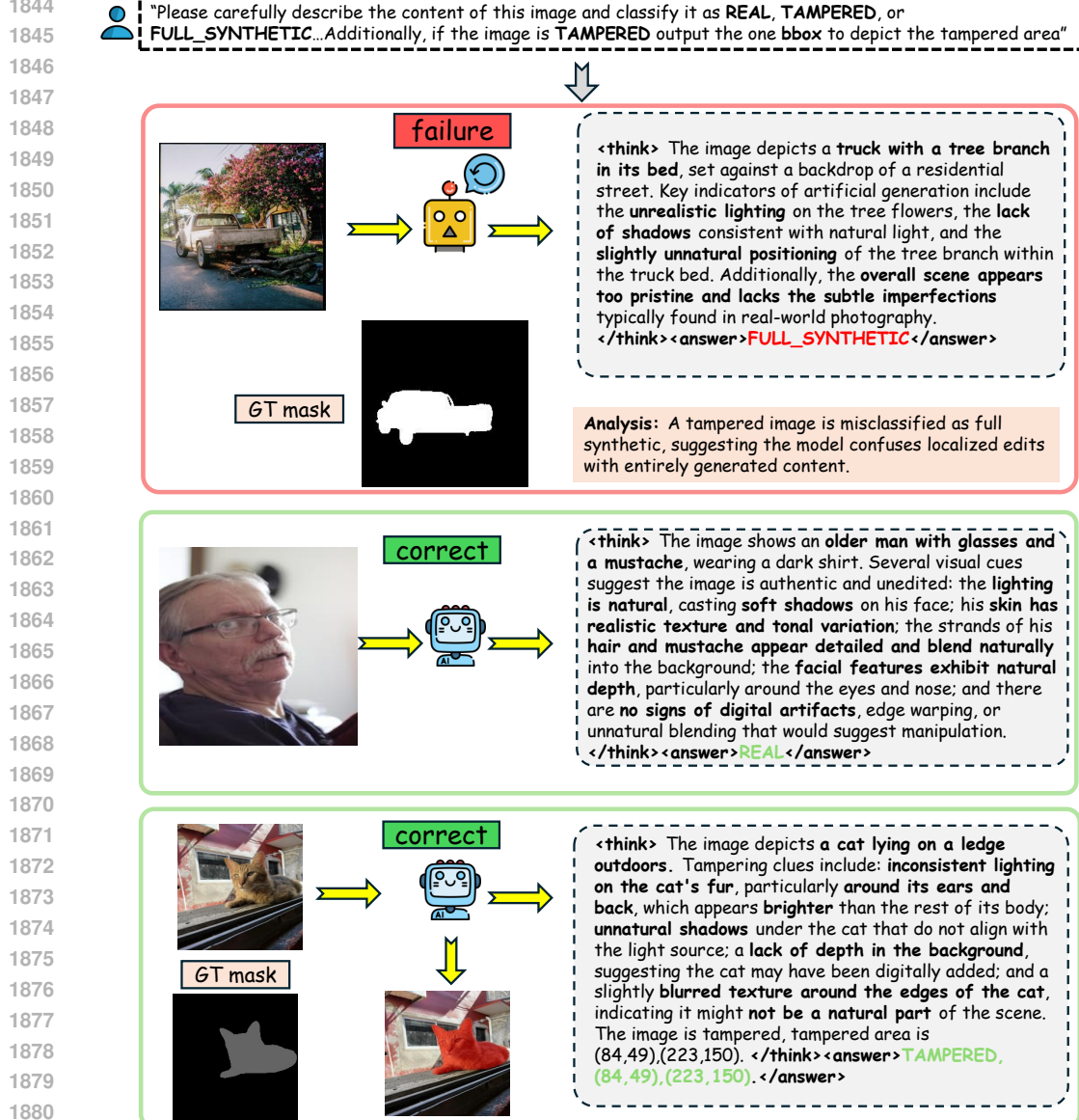
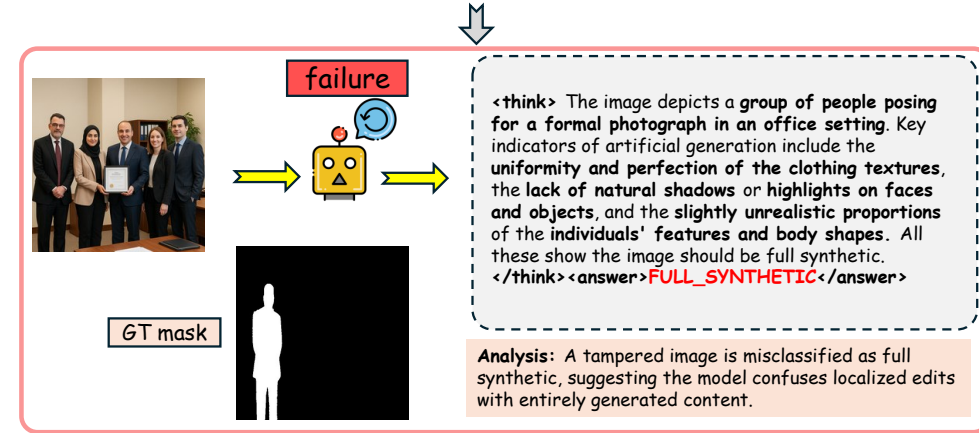


Figure 21: Qualitative results of So-Fake-R1 on the So-Fake-OOD benchmark.

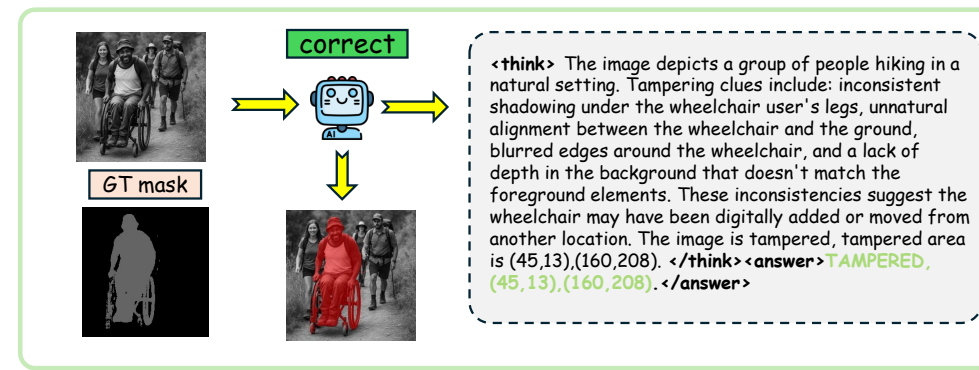
1890
1891
1892
1893
1894
1895
1896
1897

1898  "Please carefully describe the content of this image and classify it as **REAL**, **TAMPERED**, or **FULL_SYNTHETIC**... Additionally, if the image is **TAMPERED** output the one **bbox** to depict the tampered area"

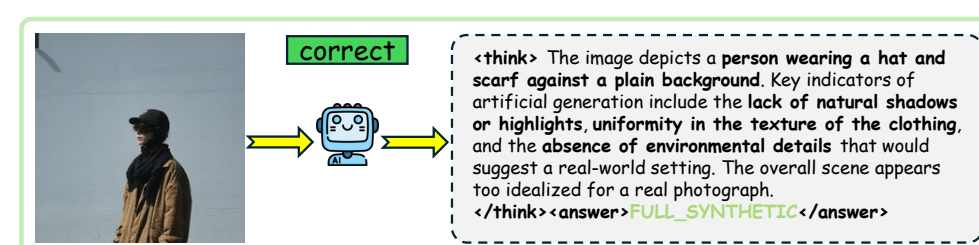
1900
1901
1902
1903
1904
1905
1906
1907
1908
1909
1910
1911
1912
1913



1914
1915
1916
1917
1918
1919
1920
1921
1922
1923
1924
1925



1926
1927
1928
1929
1930
1931
1932
1933



1934
1935
1936
1937
1938
1939
1940
1941
1942
1943

Figure 22: Qualitative results of So-Fake-R1 on the So-Fake-OOD benchmark.

1944
1945
1946
1947
1948
1949
1950
1951

1952  "Please carefully describe the content of this image and classify it as **REAL**, **TAMPERED**, or **FULL_SYNTHETIC**... Additionally, if the image is **TAMPERED** output the one **bbox** to depict the tampered area"

1954
1955

1956
1957
1958
1959
1960
1961
1962
1963

1964
1965
1966
1967
1968
1969
1970
1971
1972
1973
1974

1975
1976
1977
1978
1979
1980
1981
1982
1983
1984
1985
1986
1987
1988
1989

1990 Figure 23: Qualitative results of So-Fake-R1 on the So-Fake-OOD benchmark.

1991
1992
1993
1994
1995
1996
1997



